Inorg. Chem. **2006**, *45*, 10859–10872

Mixed-Metal Cluster Chemistry. 29. Core Expansion and Ligand-Driven Metal Exchange at Group 6–Iridium Clusters[1]

Alistair J. Usher,[†] Nigel T. Lucas,[†] Gulliver T. Dalton,[†] Michael D. Randles,[†] Lydie Viau,[†] Mark G. Humphrey,*[,†] Simon Petrie,[†] Robert Stranger,[†] Anthony C. Willis,[‡] and A. David Rae[‡]

Department of Chemistry, Australian National University, Canberra ACT 0200, Australia, and Research School of Chemistry, Australian National University, Canberra ACT 0200, Australia

Received September 13, 2006

Reactions of the tetrahedral clusters $MoIr_3(\mu\text{-}CO)_3(CO)_8(\eta\text{-}L)$ (L = C_5HMe_4, C_5Me_5) with the carbonylmetalate anions $[Mo(CO)_3(\eta\text{-}L)]^-$ afford the trigonal bipyramidal clusters $Mo_2Ir_3(\mu_3\text{-}H)(\mu\text{-}CO)_2(CO)_9(\eta\text{-}L)_2$ (L = C_5HMe_4 (**3c**), 74%; L = C_5Me_5 (**3d**), 55%) in which the group 6 metal atoms occupy the apexes; reaction of the cyclopentadienylmolybdenum-containing analogues or their cyclopentadienyltungsten-containing homologues failed to afford analogous products. Reactions of $MIr_3(\mu\text{-}CO)_3(CO)_8(\eta\text{-}C_5H_5)$ (M = Mo, W) with $[M(CO)_3(\eta\text{-}L)]^-$ (L = C_5HMe_4, C_5Me_5) afford the core-expanded heteroapex clusters $M_2Ir_3(\mu_3\text{-}H)(\mu\text{-}CO)_2(CO)_9(\eta\text{-}C_5H_5)(\eta\text{-}L)$ (M = Mo, L = C_5HMe_4 (**5c**), 9%, L = C_5Me_5 (**5d**), 4%; M = W, L = C_5Me_5 (**6d**), 5%) in low yield, together with the homoapex clusters $M_2Ir_3(\mu_3\text{-}H)(\mu\text{-}CO)_2(CO)_9(\eta\text{-}L)_2$ (M = Mo, L = C_5HMe_4 (**3c**), 81%, L = C_5Me_5 (**3d**), 60%; M = W, L = C_5Me_5 (**4d**), 5%) in much higher yield for the Mo-containing examples. The identities of clusters **3c**,**d**, **4d**, and **5c,d** have been confirmed by single-crystal X-ray diffraction studies, with the same disposition of ligands about the trigonal bipyramidal cluster cores being observed in each case, a ligand arrangement that has been examined by complementary density functional theory studies. While cluster **5d** is accessible as above, no reaction is observed from $MoIr_3(\mu\text{-}CO)_3(CO)_8(\eta\text{-}C_5Me_5)$ and $[M(CO)_3(\eta\text{-}C_5H_5)]^-$. Treating $MoIr_3(\mu\text{-}CO)_3(CO)_8(\eta\text{-}C_5H_5)$ with 1 equiv of $[M(CO)_3(\eta\text{-}C_5Me_5)]^-$ affords **5d** as the major product, a further 1 equiv affording some $MoIr_3(\mu\text{-}CO)_3(CO)_8(\eta\text{-}C_5Me_5)$ and a third 1 equiv giving a good yield of **3d**. This is consistent with reaction proceeding by apex fragment addition, followed by apex fragment elimination, and finally a further apex fragment addition, the homometallic incoming apexes being distinguished from the departing vertices by their highly methylated cyclopentadienyl ligands. Spectroscopic data suggest that the electron density at these disparate-metal-containing cluster cores is tunable by progressive (conceptual) cyclopentadienyl alkylation.

Introduction

Mixed-metal clusters are of considerable interest for a variety of reasons: for example, coupling an electropositive metal and an electronegative metal to form a polar metal−metal bond may enhance organic substrate activation, metalloselectivity of reagents can potentially lead to greater stereochemical control than is possible with homometallic clusters, activation energies for ligand fluxionality can be influenced by the presence of a heterometallic atom (and the heterometallic environment can thereby facilitate discrimination between fluxional processes when more than one such process is operative), and clusters coupling early to mid-transition metals with late transition metals may be effective precursors to catalysts for a range of heterogeneously catalyzed transformations. Mixed-metal clusters incorporating disparate metals ("very mixed" metal clusters) are of particular interest, because some of the aforementioned properties will be maximized in such a cluster environment.[2] Although a large number of low nuclearity (tri- and tetranuclear) disparate metal-containing clusters exist, there are

* To whom correspondence should be addressed. E-mail: Mark.Humphrey@anu.edu.au. Ph: +61 2 6125 2927. Fax: +61 2 6125 0760.

[†] Department of Chemistry.

[‡] Research School of Chemistry.

(1) Part 28: Dalton, G. T.; Viau, L.; Waterman, S. M.; Humphrey, M. G.; Bruce, M. I.; Low, P. J.; Roberts, R. L.; Willis, A. C.; Koutsantonis, G. A.; Skelton, B. W.; White, A. H. *Inorg. Chem.* **2005**, *44*, 3261.

(2) Waterman, S. M.; Lucas, N. T.; Humphrey, M. G. In *Advances in Organometallic Chemistry*; Hill, A., West, R., Eds.; Academic Press: New York, 2000; Vol. 46, p 47.

10.1021/ic061736l CCC: $33.50
Published on Web 12/02/2006

few medium- or high-nuclearity (M_n, $n \geq 5$) examples and the paucity of general high-yielding routes into such compounds has frustrated development of their chemistry and examination of their materials properties.[2]

One of the most efficient routes into clusters of this type is by way of "metal exchange" reactions (those in which one or more metal−ligand groups of a cluster are replaced by a different metal−ligand group to afford a new cluster containing the same total number of metal atoms),[3] a procedure developed principally by Vahrenkamp and coworkers. However, as was mentioned above, most examples involve trinuclear clusters.[4] $Co_3(\mu_3\text{-CR})(CO)_9$ are the most common precursors utilized in the metal exchange reactions reported thus far, because the $Co(CO)_3$ unit is the most readily displaced group in metal exchange reactions.[5] Although treating such trinuclear clusters with (for example) molybdenum, tungsten, or nickel complexes usually induces metal exchange, cluster expansion sometimes results: reaction of $MoCo_2(\mu_3\text{-}CCO_2Pr^i)(CO)_8(\eta\text{-}C_5H_5)$, $MoNi_2(\mu_3\text{-}CCO_2Pr^i)(CO)_2(\eta\text{-}C_5H_5)_3$, or $MoCo_2(\mu_3\text{-}CCO_2Pr^i)(\mu\text{-CO})(CO)_2(\eta\text{-}C_5H_5)_3$ with $Fe_2(\mu\text{-CO})_3(CO)_6$ forms $MoFeCo_2(\mu_3\text{-}CCO_2Pr^i)(CO)_{11}(\eta\text{-}C_5H_5)$, $MoFeNi_2(\mu_3\text{-}CCO_2Pr^i)(CO)_5(\eta\text{-}C_5H_5)_3$, and $MoFeCo_2(\mu_3\text{-}CCO_2Pr^i)(CO)_5(\eta\text{-}C_5H_5)_3$, respectively,[5e] photolysis of $MRuCo(\mu_3\text{-}\eta^2\text{-}MeC_2Me)(CO)_8(\eta\text{-}C_5H_5)$ (M = Mo) in the presence of $Fe_2(\mu\text{-CO})_3(CO)_6$ affords $MoFeRuCo(\mu_3\text{-}\eta^2\text{-}MeC_2Me)(CO)_{10}(\eta\text{-}C_5H_5)$, and both the molybdenum and tungsten-containing clusters react with $Rh(CO)_2(\eta\text{-}C_5H_5)$ to form $MRuCoRh(\mu_3\text{-}\eta^2\text{-}MeC_2Me)(CO)_9(\eta\text{-}C_5H_5)_2$ (M = Mo, W).[6]

Almost all examples of metal exchange thus far have involved replacement of one ligated metal fragment with another containing a different metal atom, but low-yielding exceptions (i.e., corresponding to a formal ligand exchange only) have been noted: $MoCo_2(\mu_3\text{-CR})(CO)_8\{\eta\text{-}C_5H_4C(O)Me\}$ (R = Ph, CO_2Et) reacts with $[Mo(CO)_3(\eta^5\text{-L})]^-$ (L = C_9H_7, C_5H_5) to afford $MoCo_2(\mu_3\text{-CR})(CO)_8(\eta^5\text{-L})$ (7−47%),[7,8] the linked diclusters $\{MoCo_2(\mu_3\text{-CR})(CO)_8\}_2(\mu\text{-}C_5H_4C(O)C_6H_4\text{-}4\text{-}C(O)C_5H_4)$ (R = CO_2Et, Ph) react with $[Mo(CO)_3(\eta\text{-}C_5H_4R')]^-$ (R′ = H, C(O)Me, CO_2Et) to give vertex-exchanged monoclusters (30−39%),[9] and linked diclusters react with linked dicluster dianions to give mixtures of linked mono-, di-, and tricluster species.[9]

Metal exchange procedures to afford mixed-metal clusters with disparate metals have been utilized most frequently with trinuclear clusters, and reactions involving tetranuclear clusters have also been successful.[10] Metal exchange at higher nuclearity examples has yet to be exploited—it has been suggested that the preponderance of trinuclear clusters is due to the significant stabilization imparted by the presence of the capping main group unit in the tetrahedral cores.[4] We report herein syntheses of medium-nuclearity very-mixed metal clusters by an unusual combination of core expansion and metal exchange upon reacting $MIr_3(CO)_{11}(\eta\text{-L})$ (M = Mo, W; L = C_5H_5, C_5HMe_4, C_5Me_5) with $[M(CO)_3(\eta\text{-L})]^-$ (M = Mo, W; L = C_5HMe_4, C_5Me_5), the metal exchange being a remarkable "ligand-driven" process, together with comprehensive theoretical, structural, and spectroscopic studies of the resultant species, and studies clarifying aspects of the reaction mechanism.

Experimental Section

General Conditions and Reagents. Reactions were performed under an atmosphere of nitrogen using standard Schlenk techniques. Product clusters proved indefinitely stable in air as solids and for at least short periods of time in solution, and thus no special precautions were taken to exclude air in their workup. Solvents used in reactions were AR grade and distilled under nitrogen using standard methods: CH_2Cl_2 over CaH_2; THF over sodium benzophenone ketyl. All other solvents were used as received. Petroleum spirit refers to a fraction of boiling range 60−80 °C. Cluster products were purified by preparative thin-layer chromatography (TLC) on 20 × 20 cm glass plates coated with Merck GF_{254} silica gel (0.5 mm). Analytical TLC was conducted on aluminum sheets coated with 0.25 mm Merck GF_{254} silica gel. Cyclopentadiene (Aldrich) was distilled from dicyclopentadiene before use. Pentamethylcyclopentadiene, tetramethylcyclopentadiene (mixture of isomers), molybdenum hexacarbonyl, tungsten hexacarbonyl, potassium hydride (30% dispersion in mineral oil), magnesium sulfate, and sodium hydride (60% dispersion in mineral oil) (Aldrich) were used as received. Literature procedures were used to synthesize $Na[M(CO)_3(\eta\text{-}C_5H_5)]$ (M = Mo, W), $Li[Mo(CO)_3(\eta\text{-}C_5H_{5-n}Me_n)]$ (n = 0, 4, 5), $K[Mo(CO)_2(PPh_3)(\eta\text{-}C_5H_5)]$,[11] $WIr_3(CO)_{11}(\eta\text{-}C_5H_5)$,[12] $MoIr_3(\mu\text{-CO})_3(CO)_8(\eta\text{-}C_5H_5)$ (**2a**),[13] $MoIr_3(\mu\text{-CO})_3(CO)_8(\eta\text{-}C_5HMe_4)$ (**2c**), $MoIr_3(\mu\text{-CO})_3(CO)_8(\eta\text{-}C_5Me_5)$ (**2d**),[14] $MoIr_3(CNBu^t)(CO)_{10}(\eta\text{-}C_5Me_5)$,[15] and $Mo_2Ir_2(\mu\text{-CO})_3(CO)_7(\eta\text{-}C_5H_5)_2$ (**1a**).[16] *n*-Butyllithium (solution in hexane, Aldrich) was

(3) Shriver, D. F.; Kaesz, H. D.; Adams, R. D. *The Chemistry of Metal Cluster Complexes*; VCH: New York, 1990.
(4) Vahrenkamp, H. *Comments Inorg. Chem.* **1985**, *4*, 253.
(5) (a) Clark, D. T.; Sutin, K. A.; McGlinchey, M. J. *Organometallics* **1989**, *8*, 155. (b) Sutin, K. A.; Kolis, J. W.; Mlekuz, M.; Bougeard, P.; Sayer, B. G.; Quilliam, M. A.; Faggiani, R.; Lock, C. J. L.; McGlinchey, M. J.; Jaouen, G. *Organometallics* **1987**, *6*, 439. (c) Beurich, H.; Blumhofer, R.; Vahrenkamp, H. *Chem. Ber.* **1982**, *115*, 2409. (d) Schacht, H.-T.; Vahrenkamp, H. *Chem. Ber.* **1989**, *122*, 2239. (e) Mlekuz, M.; Bougeard, P.; Sayer, B. G.; Faggiani, R.; Lock, C. J. L.; McGlinchey, M. J.; Jaouen, G. *Organometallics* **1985**, *4*, 2046. (f) Jensen, S.; Robinson, B. H.; Simpson, J. *J. Chem. Soc. Chem. Commun.* **1983**, 1081. (g) Wu, H.-P.; Yin, Y.-Q.; Huang, X.-Y.; Yu, K.-B. *J. Organomet. Chem.* **1995**, *498*, 119. (h) Sutin, K. A.; Li, L.; Frampton, C. S.; Sayer, B. G.; McGlinchey, M. J. *Organometallics* **1991**, *10*, 2362. (i) Duffy, D. N.; Kassis, M. M.; Rae, A. D. *Acta Crystallogr.* **1991**, *C47*, 2343. (j) Richter, F.; Beurich, H.; Vahrenkamp, H. *J. Organomet. Chem.* **1979**, *166*, C5.
(6) Bantel, H.; Powell, A. K.; Vahrenkamp, H. *Chem. Ber.* **1990**, *123*, 677.
(7) Zhang, W.-Q.; Zhu, B.-H.; Hu, B.; Zhang, Y.-H.; Zhao, Q.-Y.; Yin, Y.-Q.; Sun, J. *J. Organomet. Chem.* **2004**, *689*, 714.
(8) Zhang, Y.-H.; Liu, P.; Xia, C.-G.; Hu, B.; Yin, Y.-Q. *J. Organomet. Chem.* **2003**, *676*, 55.
(9) Song, L.-C.; Guo, D.-S. *Pure Appl. Chem.* **2001**, *73*, 305.
(10) (a) Kaganovich, V. S.; Slovokhotov, Y. L.; Mironov, A. V.; Struchkov, Y. T.; Rybinskaya, M. I. *J. Organomet. Chem.* **1989**, *372*, 339. (b) Kuznetsov, V. F.; Bensimon, C.; Facey, G. A.; Grushin, V. V.; Alper, H. *Organometallics* **1997**, *16*, 97.
(11) Inkrott, K.; Goetze, R.; Shore, S. G. *J. Organomet. Chem.* **1978**, *154*, 337.
(12) Shapley, J. R.; Hardwick, S. J.; Foose, D. S.; Stucky, G. D. *J. Am. Chem. Soc* **1981**, *103*, 7383.
(13) Churchill, M. R.; Li, Y.-J.; Shapley, J. R.; Foose, D. S.; Uchiyama, W. S. *J. Organomet. Chem.* **1986**, *312*, 121.
(14) Lucas, N. T.; Blitz, J. P.; Petrie, S.; Stranger, R.; Humphrey, M. G.; Heath, G. A.; Otieno-Alego, V. *J. Am. Chem. Soc.* **2002**, *124*, 5139.
(15) Usher, A. J.; Humphrey, M. G.; Willis, A. C. *J. Organomet. Chem.* **2003**, *682*, 41.
(16) Lucas, N. T.; Humphrey, M. G.; Hockless, D. C. R. *J. Organomet. Chem.* **1997**, *535*, 175.

titrated with diphenylacetic acid in diethyl ether prior to each use to determine its exact concentration.[17]

Instrumentation. Infrared spectra were recorded on a Perkin-Elmer System 2000 FT-IR using a CaF_2 cell. Spectral features are reported in cm^{-1}. All solution IR spectra were recorded in AR grade cyclohexane, THF or CH_2Cl_2 solvent. ^1H NMR spectra were recorded on a Varian Gemini-300 spectrometer at 300 MHz in $CDCl_3$ (Cambridge Isotope Laboratories) and referenced to residual nondeuterated solvent (δ 7.24). Unit resolution SI mass spectra were recorded on a VG Autospec instrument at the Research School of Chemistry, Australian National University. Unit resolution FAB mass spectra were recorded on an AutospecE instrument at the University of Western Australia. All MS are reported in the following form: *m*/*z* (assignment, relative intensity). UV−vis spectra were recorded on a Cary 5 spectrophotometer. Microanalyses were carried out by the Microanalysis Service Unit in the Research School of Chemistry, ANU.

Reaction of $MoIr_3(\mu\text{-}CO)_3(CO)_8(\eta\text{-}C_5HMe_4)$ with $Li[Mo(CO)_3(\eta\text{-}C_5HMe_4)]$ (Method A). A solution of $Li[Mo(CO)_3(\eta\text{-}C_5HMe_4)]$ was prepared from *n*-butyllithium in hexane (0.50 mL, 2.0 M, 1.0 mmol), tetramethylcyclopentadiene (0.25 mL, 200 mg, 1.64 mmol), and $Mo(CO)_6$ (270 mg, 1.02 mmol) in THF (20 mL). An aliquot (1.50 mL, ca. 0.075 mmol) of this solution was added to a second Schlenk flask containing $MoIr_3(\mu\text{-}CO)_3(CO)_8(\eta\text{-}C_5HMe_4)$ (**2c**) (31.4 mg, 0.0285 mmol) in THF (5 mL), and the resultant mixture was stirred at room temperature for 2 h. Monitoring by solution IR indicated that the amount of **2c** had decreased slightly. The mixture was heated at reflux for 1.5 h, and an examination of the solution IR after this time indicated significant depletion of **2c**. Another aliquot (1.0 mL) of the $Li[Mo(CO)_3(\eta\text{-}C_5HMe_4)]$ solution was added before refluxing was continued a further 3 h, after which time IR confirmed that all the starting cluster had been consumed. The solution was cooled, acetic acid (0.2 mL) was added with stirring, and the reaction mixture transferred to a small separating funnel using CH_2Cl_2 (50 mL). Following extraction with water, the organic phase was dried with $MgSO_4$, filtered, and taken to dryness on a rotary evaporator. The brown residue was dissolved in CH_2Cl_2 (ca 2 mL) and applied to preparative TLC plates. Elution with CH_2Cl_2/petroleum spirit (1/1) gave four bands. The contents of the first ($R_f = 0.83$, brown), second ($R_f = 0.71$, red-brown) and fourth ($R_f = 0.51$, brown) bands appeared to be in trace amounts, and they were not isolated. The contents of the third and major band ($R_f = 0.59$) were extracted with CH_2Cl_2 and recrystallized from CH_2Cl_2/ethanol at 3 °C to afford brown crystals of $Mo_2Ir_3(\mu_3\text{-}H)(\mu\text{-}CO)_2(CO)_9(\eta\text{-}C_5HMe_4)_2$ (**3c**) (28.0 mg, 0.0212 mmol, 74%). IR (CH_2Cl_2): ν(CO) 2047 w, 2017 vs, 1981 s, 1909 m, 1778 w, 1748 m cm^{-1}. UV−vis (THF): 359 (10.4), 407 sh (7.0), 451 sh (5.0), 595 sh (1.1) nm (10^3 L mol^{-1} cm^{-1}). ^1H-NMR ($CDCl_3$): δ 4.75 (s, 2H, C_5HMe$_4$), 2.02, 2.01 (2 × s, 2 × 12H, C_5HMe_4), −5.49 (s, 1H, MH). MS (SI): 1319 ($[M]^+$, 47), 1291 ($[M - CO]^+$, 59), 1263 ($[M - 2CO]^+$, 27), 1235 ($[M - 3CO]^+$, 57), 1207 ($[M - 4CO]^+$, 40), 1179 ($[M - 5CO]^+$, 75), 1150 ($[M - 6CO - H]^+$, 42), 1122 ($[M - 7CO - H]^+$, 44), 1094 ($[M - 8CO - H]^+$, 41), 1066 ($[M - 9CO - H]^+$, 58), 1051 ($[M - 9CO - MeH]^+$, 51), 1038 ($[M - 10CO - H]^+$, 55), 1023 ($[M - 10CO - MeH]^+$, 82), 1010 ($[M - 11CO - H]^+$, 64). Anal. Calcd for $C_{29}H_{27}Ir_3Mo_2O_{11}$: C, 26.39; H, 2.06. Found: C, 26.61; H, 2.36.

Reaction of $MoIr_3(\mu\text{-}CO)_3(CO)_8(\eta\text{-}C_5H_5)$ with $Na[Mo(CO)_3(\eta\text{-}C_5H_5)]$ (Method B). A solution of $Na[Mo(CO)_3(\eta\text{-}C_5H_5)]$ was prepared from NaH (60% dispersion in mineral oil, 57 mg, 1.42 mmol), cyclopentadiene (0.3 mL, 3.0 mmol), and $Mo(CO)_6$ (370 mg, 1.40 mmol) in THF. A solution of $MoIr_3(\mu\text{-}CO)_3(CO)_8(\eta\text{-}C_5H_5)$ (**2a**) (41.8 mg, 0.040 mmol) in THF (20 mL) was stirred with 2 mL of crude $Na[Mo(CO)_3(\eta\text{-}C_5H_5)]$ solution (ca. 0.28 mmol) for 2 h, at which time solution IR showed no depletion of starting material. The solution was then heated to 45 °C for 2 h, at which time solution IR showed a slight reduction of starting material. Heating was continued for a further 14 h, at which time solution IR showed destruction of starting material and analytical TLC failed to show formation of any tractable products.

Reaction of $MoIr_3(\mu\text{-}CO)_3(CO)_8(\eta\text{-}C_5Me_5)$ with $Li[Mo(CO)_3(\eta\text{-}C_5Me_5)]$ (1:1.5). Following method A, a solution of $MoIr_3(\mu\text{-}CO)_3(CO)_8(\eta\text{-}C_5Me_5)$ (**2d**) (15 mg, 0.013 mmol) in THF (20 mL) was stirred under reflux with 1.8 mL of crude $Li[Mo(CO)_3(\eta\text{-}C_5Me_5)]$ solution (ca. 0.02 mmol) for 5 h, and then acetic acid (0.15 mL) was added. Preparative TLC (1:1 CH_2Cl_2/petroleum spirit eluant) gave three bands. The first and third bands appeared to be in trace amounts and were not isolated. The contents of the second and major band ($R_f = 0.54$) were crystallized from CH_2Cl_2/EtOH to afford dark brown crystals identified as $Mo_2Ir_3(\mu_3\text{-}H)(\mu\text{-}CO)_2(CO)_9(\eta\text{-}C_5Me_5)_2$ (**3d**) (9.9 mg, 0.007 mmol, 55%). IR (CH_2Cl_2): ν(CO) 2044 m, 2014 vs, 1979 s, 1892 m, 1775 m, 1746 s cm^{-1}. ^1H NMR ($CDCl_3$): δ 1.97 (s, 30H, C_5Me_5), −5.44 (s, 1H, M*H*) ppm. MS (FAB): 1349 ($[M]^+$, 38), 1321 ($[M - CO]^+$, 25), 1293 ($[M - 2CO]^+$, 13), 1265 ($[M - 3CO]^+$, 47), 1237 ($[M - 4CO]^+$, 21), 1209 ($[M - 5CO]^+$, 100), 1181 ($[M - 6CO]^+$, 34), 1153 ($[M - 7CO]^+$, 27), 1125 ($[M - 8CO]^+$, 25), 1123 ($[M - 7CO - 2Me]^+$, 25), 1095 ($[M - 8CO - 2Me]^+$, 47), 1065 ($[M - 8CO - 4Me]^+$, 72). Anal. Calcd for $C_{31}H_{31}Ir_3Mo_2O_{11}$: C, 27.62; H, 2.32. Found: C, 27.62; H, 2.35.

Reaction of $WIr_3(CO)_{11}(\eta\text{-}C_5H_5)$ with $Na[W(CO)_3(\eta\text{-}C_5H_5)]$. Following method B, a solution of $Na[W(CO)_3(\eta\text{-}C_5H_5)]$ in THF (3 mL of 0.04 M, ca. 0.1 mmol) and a solution of $WIr_3(CO)_{11}(\eta\text{-}C_5H_5)$ (29 mg, 0.026 mmol) in THF (15 mL) were heated at reflux for 48 h, after which time acetic acid (3 drops) was added. Preparative TLC gave no tractable products.

Reaction of $MoIr_3(\mu\text{-}CO)_3(CO)_8(\eta\text{-}C_5H_5)$ with $Li[Mo(CO)_3(\eta\text{-}C_5HMe_4)]$. Following method A, a solution of $MoIr_3(\mu\text{-}CO)_3(CO)_8(\eta\text{-}C_5H_5)$ (**2a**) (21.3 mg, 0.020 mmol) in THF (20 mL) was stirred under reflux with 2.8 mL of crude $Li[Mo(CO)_3(\eta\text{-}C_5HMe_4)]$ solution (ca. 0.14 mmol) for 4 h and cooled, and then acetic acid (0.15 mL) was added. Preparative TLC (1:1 CH_2Cl_2/petroleum spirit eluant) gave two major bands and a number of traces. The contents of the first and major band ($R_f = 0.53$) contained $Mo_2Ir_3(\mu_3\text{-}H)(\mu\text{-}CO)_2(CO)_9(\eta\text{-}C_5HMe_4)_2$ (**3c**) (21.5 mg, 0.017 mmol, 81%), identified by solution IR and ^1H NMR spectroscopy. The contents of the second major band ($R_f = 0.36$) were crystallized from CH_2Cl_2/EtOH to afford dark brown crystals identified as $Mo_2Ir_3(\mu_3\text{-}H)(\mu\text{-}CO)_2(CO)_9(\eta\text{-}C_5H_5)(\eta\text{-}C_5HMe_4)$ (**5c**) (2.3 mg, 0.002 mmol, 9%). IR (CH_2Cl_2): ν(CO) 2051 w, 2022 vs, 1987 s, 1907 w, 1785 w, 1755 m cm^{-1}. ^1H NMR ($CDCl_3$): δ 5.15 (s, 5H, C_5H_5), 5.07 (s, 1H, C_5HMe$_4$), 2.07, 2.03 (2 × s, 2 × 6H, C_5HMe_4), −5.63 (s, 1H, M*H*) ppm. MS (SI): 1265 ($[M]^+$, 35), 1237 ($[M - CO]^+$, 35), 1209 ($[M - 2CO]^+$, 13), 1181 ($[M - 3CO]^+$, 36), 1153 ($[M - 4CO]^+$, 20), 1125 ($[M - 5CO]^+$, 24), 1097 ($[M - 6CO]^+$, 17). Microanalysis could not be obtained due to the small sample size.

Reaction of $MoIr_3(\mu\text{-}CO)_3(CO)_8(\eta\text{-}C_5H_5)$ with $Li[Mo(CO)_3(\eta\text{-}C_5Me_5)]$ (1:2.3). Following method A, a solution of $MoIr_3(\mu\text{-}CO)_3(CO)_8(\eta\text{-}C_5H_5)$ (**2a**) (50 mg, 0.048 mmol) in THF (20 mL) was stirred under reflux with 10 mL of crude $Li[Mo(CO)_3(\eta\text{-}C_5Me_5)]$ solution (ca. 0.11 mmol) for 5 h, and then acetic acid (0.15 mL) was added. Preparative TLC (1:1 CH_2Cl_2/petroleum spirit eluant) gave four bands. The first and fourth bands were in trace amounts and could not be isolated. The contents of the second and

(17) Kofron, W. G.; Baclowski, L. M. *J. Org. Chem.* **1976**, *41*, 1879.

major band were identified as $Mo_2Ir_3(\mu_3\text{-}H)(\mu\text{-}CO)_2(CO)_9(\eta\text{-}C_5Me_5)_2$ (**3d**) (38.6 mg, 0.029 mmol, 60%) by solution IR and ^1H NMR spectroscopy. The contents of the third band were crystallized from CH_2Cl_2/EtOH to afford brown crystals identified as $Mo_2Ir_3(\mu_3\text{-}H)(\mu\text{-}CO)_2(CO)_9(\eta\text{-}C_5H_5)(\eta\text{-}C_5Me_5)$ (**5d**) (2.5 mg, 0.002 mmol, 4%). IR (CH_2Cl_2): ν(CO) 2048 w, 2020 vs, 1985 m, 1910 w, 1753 m cm^{-1}. ^1H NMR ($CDCl_3$): δ 5.13 (s, 5H, C_5H_5), 2.03 (s, 15H, C_5Me_5), −5.56 (s, 1H, M*H*) ppm. MS (FAB): 1278 ($[M]^+$, 92), 1250 ($[M - CO]^+$, 100), 1222 ($[M - 2CO]^+$, 14), 1194 ($[M - 3CO]^+$, 71), 1166 ($[M - 4CO]^+$, 39), 1138 ($[M - 5CO]^+$, 52), 1110 ($[M - 6CO]^+$, 41), 1082 ($[M - 7CO]^+$, 46), 1054 ($[M - 8CO]^+$, 40), 1026 ($[M - 9CO]^+$, 49). Microanalysis could not be obtained due to the small sample size.

Reaction of $MoIr_3(\mu\text{-}CO)_3(CO)_8(\eta\text{-}C_5H_5)$ with $Li[Mo(CO)_3(\eta\text{-}C_5Me_5)]$ (1:1). Following method A, a solution of $MoIr_3(\mu\text{-}CO)_3(CO)_8(\eta\text{-}C_5H_5)$ (**2a**) (56.1 mg, 0.0536 mmol) in THF (15 mL) was stirred under reflux with 1.1 mL of crude $Li[Mo(CO)_3(\eta\text{-}C_5Me_5)]$ solution (ca. 0.050 mmol) for 4.5 h, and then acetic acid (0.15 mL) was added. Preparative TLC (1:1 CH_2Cl_2/petroleum spirit eluant) gave three bands. The contents of the first band were identified as $MoIr_3(\mu\text{-}CO)_3(CO)_8(\eta\text{-}C_5Me_5)$ (**2d**) (4.5 mg, 0.0043 mmol, 8%) by solution IR and ^1H NMR. The contents of the second band were identified as $Mo_2Ir_3(\mu_3\text{-}H)(\mu\text{-}CO)_2(CO)_9(\eta\text{-}C_5Me_5)_2$ (**3d**) (8.2 mg, 0.0061 mmol, 11%) by solution IR and ^1H NMR spectroscopy. The contents of the third band were identified as $Mo_2Ir_3(\mu_3\text{-}H)(\mu\text{-}CO)_2(CO)_9(\eta\text{-}C_5H_5)(\eta\text{-}C_5Me_5)$ (**5d**) (19.9 mg, 0.0156 mmol, 31%) by solution IR and ^1H NMR spectroscopy and a satisfactory microanalysis. Anal. Calcd for $C_{26}H_{21}Ir_3Mo_2O_{11}$: 24.44; H, 1.66. Found: C, 24.09; H, 1.68.

Reaction of $MoIr_3(\mu\text{-}CO)_3(CO)_8(\eta\text{-}C_5Me_5)$ with $Na[Mo(CO)_3(\eta\text{-}C_5H_5)]$. Following method B, a solution of $MoIr_3(\mu\text{-}CO)_3(CO)_8(\eta\text{-}C_5Me_5)$ (41.8 mg, 0.040 mmol) in THF (20 mL) was stirred with 2 mL of crude $Na[Mo(CO)_3(\eta\text{-}C_5H_5)]$ solution (ca 0.3 mmol) for 2 h, at which time solution IR showed no depletion of starting material. The solution was heated to reflux for 24 h, and periodic monitoring by solution IR and analytical TLC failed to show the formation of any tractable products.

Reaction of $WIr_3(CO)_{11}(\eta\text{-}C_5H_5)$ with $Li[W(CO)_3(\eta\text{-}C_5Me_5)]$. Following method A, a solution of $Li[W(CO)_3(\eta\text{-}C_5Me_5)]$ in THF (1.2 mL of a 0.095 M solution, 0.11 mmol) and a solution of $WIr_3(CO)_{11}(\eta\text{-}C_5H_5)$ (38.4 mg, 0.0339 mmol) in THF (15 mL) were heated at reflux for 18 h, after which acetic acid (10 drops) was added. Preparative TLC (1:1 CH_2Cl_2/petroleum spirit eluant) gave eight bands. The first five bands (orange, orange, yellow, purple, and brown, respectively) were in minor amounts and were not isolated. The contents of the sixth band (brown) were crystallized from CH_2Cl_2/EtOH at 3 °C to afford dark brown crystals, identified as $W_2Ir_3(\mu_3\text{-}H)(\mu\text{-}CO)_2(CO)_9(\eta\text{-}C_5Me_5)_2$ (**4d**) (2.4 mg, 0.0016 mmol, 5%). IR (CH_2Cl_2): ν(CO) 2045 w, 2013 vs, 1978 m, 1895 br, 1736 br cm^{-1}. ^1H NMR ($CDCl_3$): δ 2.10 (s, 30H, Me), −1.83 (s, 1H, MH) ppm. MS (SI): 1524 ($[M]^+$, 100), 1496 ($[M - CO]^+$, 48), 1468 ($[M - 2CO]^+$, 12), 1440 ($[M - 3CO]^+$, 81). The contents of the seventh band (brown) were crystallized from CH_2Cl_2/EtOH at 3 °C to afford dark brown crystals identified as $W_2Ir_3(\mu_3\text{-}H)(\mu\text{-}CO)_2(CO)_9(\eta\text{-}C_5H_5)(\eta\text{-}C_5Me_5)]$ (**6d**) (2.4 mg, 0.0017 mmol, 5%). IR (CH_2Cl_2): ν(CO) 2048 w, 2018 vs, 1984 m, 1913 br, 1742 br cm^{-1}. ^1H NMR ($CDCl_3$): δ 5.20 (s, 5H, C_5H_5), 2.17 (s, 15H, C_5Me_5), −2.00 (s, 1H, MH) ppm. MS (SI): 1454 ($[M]^+$, 52), 1426 ($[M - CO]^+$, 100). Microanalyses could not be obtained due to the small sample size.

Reaction of $WIr_3(CO)_{11}(\eta\text{-}C_5H_5)$ with $Li[Mo(CO)_3(\eta\text{-}C_5Me_5)]$. Following method A, a solution of $WIr_3(CO)_{11}(\eta\text{-}C_5H_5)$ (30.0 mg, 0.026 mmol) in THF (15 mL) and a 5 mL aliquot of $Li[Mo(CO)_3(\eta\text{-}C_5Me_5)]$ solution (ca. 0.05 mmol) were heated at reflux for 21 h, another 5 mL aliquot of $Li[Mo(CO)_3(\eta\text{-}C_5Me_5)]$ solution was added and refluxing continued for 24 h, and a further 5 mL aliquot of $Li[Mo(CO)_3(\eta\text{-}C_5Me_5)]$ solution was added followed by reflux for a further 48 h. The solution was allowed to cool to room temperature, and acetic acid (2 mL) followed by CCl_4 (2 mL) was added. Workup as before (preparative TLC plates, 1:1 CH_2Cl_2/petroleum spirit eluant) gave five bands. The contents of the first band [red, probably $Mo_2(CO)_6(\eta\text{-}C_5H_5)_2$] were in trace amounts and could not be isolated. The contents of the second band (R_f = 0.83) were identified as unreacted $WIr_3(CO)_{11}(\eta\text{-}C_5H_5)$ (ca. 0.1 mg) by solution IR and ^1H NMR spectroscopy. The contents of the third band (R_f = 0.69) were in trace amounts and could not be isolated. The contents of the fourth and major band (R_f = 0.58) were identified as $Mo_2Ir_3(\mu_3\text{-}H)(\mu\text{-}CO)_2(CO)_9(\eta\text{-}C_5Me_5)_2$ (**3d**) (14.7 mg, 0.011 mmol, 42%) by solution IR and ^1H NMR spectroscopy. The orange contents of the fifth band (R_f = 0.48) were not identified.

Reaction of $Mo_2Ir_2(\mu\text{-}CO)_3(CO)_7(\eta\text{-}C_5H_5)_2$ with $Li[Mo(CO)_3(\eta\text{-}C_5Me_5)]$. Following method B, a solution of $Mo_2Ir_2(\mu\text{-}CO)_3(CO)_7(\eta\text{-}C_5H_5)_2$ (**1a**) (32 mg, 0.032 mmol) in THF (15 mL) and a 4 mL aliquot of the $Li[Mo(CO)_3(\eta\text{-}C_5Me_5)]$ solution (ca. 0.04 mmol) were stirred at room temperature for 3 h and then heated at reflux for 3 h. Preparative TLC (multiple development, 5:2 CH_2Cl_2/petroleum spirit eluant followed by 1:1 CH_2Cl_2/petroleum ether eluant) gave 24 bands, all of which were in trace amounts and could not be isolated.

Reaction of $Mo_2Ir_3(\mu_3\text{-}H)(\mu\text{-}CO)_2(CO)_9(\eta\text{-}C_5HMe_4)_2$ with $Li[Mo(CO)_3(\eta\text{-}C_5Me_5)]$. A solution of $Mo_2Ir_3(\mu_3\text{-}H)(\mu\text{-}CO)_2(CO)_9(\eta\text{-}C_5HMe_4)_2$ (**3c**) (19.9 mg, 0.016 mmol) in THF (20 mL) and a 5 mL aliquot of a $Li[Mo(CO)_3(\eta\text{-}C_5Me_5)]$ solution (ca 0.05 mmol) were stirred at room temperature for 4 h. Monitoring the mixture by solution IR indicated no changes in the spectrum of the starting cluster, and the solution was heated to reflux for 6 h before workup (preparative TLC, 1:1 CH_2Cl_2/petroleum spirit eluant) returned unreacted $Mo_2Ir_3(\mu_3\text{-}H)(\mu\text{-}CO)_2(CO)_9(\eta\text{-}C_5HMe_4)_2$ (**3c**) (19.3 g, 0.015 mmol, 97%) identified by solution IR and ^1H NMR spectroscopy.

Reaction of $Mo_2Ir_3(\mu_3\text{-}H)(\mu\text{-}CO)_2(CO)_9(\eta\text{-}C_5H_5)(\eta\text{-}C_5Me_5)$ with $Li[Mo(CO)_3(\eta\text{-}C_5Me_5)]$. A solution of $Mo_2Ir_3(\mu_3\text{-}H)(\mu\text{-}CO)_2(CO)_9(\eta\text{-}C_5H_5)(\eta\text{-}C_5Me_5)$ (**5d**) (19.9 mg, 0.016 mmol) in THF (15 mL) and a 0.33 mL aliquot of a $Li[Mo(CO)_3(\eta\text{-}C_5Me_5)]$ solution (ca. 0.015 mmol) were refluxed for 4.5 h, and then acetic acid (0.15 mL) was added. Preparative TLC (1:1 CH_2Cl_2/petroleum spirit eluant) gave six bands. Bands 1 and 6 were in trace amounts. The contents of the second band were identified as $MoIr_3(\mu\text{-}CO)_3(CO)_8(\eta\text{-}C_5Me_5)$ (**2d**) (0.9 mg, 0.0009 mmol, 5%) by solution IR and ^1H NMR spectroscopy. The contents of the third band (1.2 mg) could not be identified. The contents of the fourth band were identified as $Mo_2Ir_3(\mu_3\text{-}H)(\mu\text{-}CO)_2(CO)_9(\eta\text{-}C_5Me_5)_2$ (**3d**) (0.9 mg, 0.00067 mmol, 4%) by solution IR and ^1H NMR spectroscopy. The contents of the fifth band were identified as unreacted $Mo_2Ir_3(\mu_3\text{-}H)(\mu\text{-}CO)_2(CO)_9(\eta\text{-}C_5H_5)(\eta\text{-}C_5Me_5)$ (**5d**) (13.3 mg, 0.0104 mmol, 67%) by solution IR and ^1H NMR spectroscopy.

Reaction of $MoIr_3(\mu\text{-}CO)_3(CNBu^t)(CO)_7(\eta\text{-}C_5Me_5)$ with $Li[Mo(CO)_3(\eta\text{-}C_5Me_5)]$. A solution of $Li[Mo(CO)_3(\eta\text{-}C_5Me_5)]$ was prepared from *n*-butyllithium in hexane (0.78 mL, 1.60 M, 1.26 mmol), pentamethylcyclopentadiene (0.20 mL, 1.28 mmol), and $Mo(CO)_6$ (344 mg, 1.30 mmol). An aliquot of this solution (5 mL, *ca* 0.05 mmol) was added to an orange solution of $MoIr_3(\mu\text{-}CO)_3(CNBu^t)(CO)_7(\eta\text{-}C_5Me_5)$ (20.5 mg, 0.018 mmol) in THF (15 mL) and the resultant solution stirred at room temperature for 17 h. Solution IR showed no reaction and the mixture was heated to reflux for 1 h, at which time solution IR showed a slight reduction of

Table 1. Crystal Data for **3c**,**d**, **4d**, and **5c**,**d**

param	**3c**	**3d**	**4d**	**5c**	**5d**
formula	$C_{29}H_{27}Ir_3Mo_2O_{11}$	$C_{31}H_{31}Ir_3Mo_2O_{11}$	$C_{31}H_{31}Ir_3O_{11}W_2$	$C_{25}H_{19}Ir_3Mo_2O_{11}$	$C_{26}H_{21}Ir_3Mo_2O_{11}$
fw	1320.07	1348.12	1523.94	1263.96	1277.98
cryst color, habit	black, prism	black, plate	black, needle	black, plate	black, plate
cryst size (mm)	0.45 × 0.23 × 0.17	0.22 × 0.14 × 0.03	0.38 × 0.10 × 0.06	0.17 × 0.17 × 0.10	0.25 × 0.22 × 0.07
cryst system	orthorhombic	monoclinic	monoclinic	orthorhombic	orthorhombic
space group	*Pnma* (No. 62)	$P2_1$ (No. 4)	$P2_1$ (No. 4)	$P2_12_12_1$ (No. 19)	*Pnma* (No. 62)
a (Å)	21.520(3)	9.14291(1)	9.1049(1)	13.0086(2)	16.1853(2)
b (Å)	15.621(2)	37.2254(3)	37.0451(4)	13.5437(2)	13.8560(2)
c (Å)	9.805(3)	15.4543(1)	15.3593(2)	16.6804(2)	13.7858(2)
β (deg)	90	92.1771(2)	92.2726(4)	90	90
V (Å^3)	3296.3(9)	5256.05(8)	5176.5(1)	2938.83(7)	3091.65(7)
Z	4	6	6	4	4
D_{calc} (g cm^{-3})	2.66	2.56	2.93	2.86	2.75
μ (mm^{-1})	12.90	12.10	18.23	14.42	13.71
radiatn	Mo Kα	Mo Kα	Mo Kα	Mo Kα	Mo Kα
T (K)	296	293	200	200	293
$2\theta_{max}$ (deg)	55.1	54.9	55.0	60.0	59.9
N_{measd}	4269	85470	74623	57030	51007
N_{unique}	3927	24032	22783	8588	4691
N_{obs} [$I > n\sigma(I)$]	2741 (2σ)	16 540 (3σ)	14 370 (3σ)	4879 (3σ)	2327 (3σ)
abs corr	analytical	integration	integration	integration	integration
T_{min}, T_{max}	0.052, 0.11	0.189, 0.701	0.060, 0.469	0.103, 0.311	0.063, 0.390
N_{param}	214	1262	137	375	193
R [$I > n\sigma(I)$]	0.030 (2σ)	0.024 (3σ)	0.054 (3σ)	0.021 (3σ)	0.024 (3σ)
R_w [$I > n\sigma(I)$]	0.032 (2σ)	0.021 (3σ)	0.059 (3σ)	0.023 (3σ)	0.027 (3σ)
$\Delta\rho_{min}$ (e Å^{-3})	−0.34	−1.47	−7.5	−1.68	−1.12
$\Delta\rho_{max}$ (e Å^{-3})	0.28	1.28	3.5	1.25	0.93

starting cluster. A further aliquot of the Li[Mo(CO)$_3$(η-C$_5$Me$_5$)] solution (5 mL) was added and heating continued for 1 h. The mixture was allowed to cool, acetic acid was added (ca 1.5 mL), and the mixture was stirred for 5 min and then reduced to dryness in vacuo. The brown residue was redissolved in a minimum of CH_2Cl_2 (ca. 1 mL) and applied to preparative TLC plates. Elution with 1:1 CH_2Cl_2/petroleum spirit gave three bands. The first band, probably Mo$_2$(CO)$_6$(η-C$_5$Me$_5$)$_2$, appeared to be in trace amounts and was not isolated. The contents of the second band (yellow, R_f = 0.61) were identified as unreacted MoIr$_3$(μ-CO)$_3$(CNBu^t)(CO)$_7$(η-C$_5$Me$_5$) (ca. 0.1 mg) by solution IR. The contents of the third band (brown, R_f = 0.37) were identified as Mo$_2$Ir$_3$(μ_3-H)(μ-CO)$_2$(CO)$_9$(η-C$_5$Me$_5$)$_2$ (**3d**) (3.4 mg, 0.002 mmol, 14%) by solution IR and ^{1}H NMR spectroscopy.

Reaction of MoIr$_3$(μ-CO)$_3$(CO)$_8$(η-C$_5$H$_5$) with K[Mo(CO)$_2$(PPh$_3$)(η-C$_5$H$_5$)]. K[Mo(CO)$_2$(PPh$_3$)(η-C$_5$H$_5$)] was prepared from Mo$_2$(CO)$_4$(PPh$_3$)$_2$(η-C$_5$H$_5$)$_2$ (150 mg, 0.16 mmol) and KH (ca. 1 g, 30% dispersion in mineral oil, 8 mmol) in THF (25 mL) over 94 h. The suspension was allowed to settle, and 10 mL of the clear orange solution was transferred to another Schlenk tube containing MoIr$_3$(μ-CO)$_3$(CO)$_8$(η-C$_5$H$_5$) (**2a**) (40.0 mg, 0.038 mmol). The bright orange solution was stirred for 1 h, at which time solution IR showed consumption of starting cluster and formation of the [Mo(CO)$_3$(η-C$_5$H$_5$)]$^-$ anion. Acetic acid (1.2 mL) was added, and the solution was reduced to dryness in vacuo; the orange residue was redissolved in a minimum of CH_2Cl_2 (ca. 1 mL) and applied to preparative TLC plates. Elution with 2:1 CH_2Cl_2/petroleum spirit gave two bands. The first band (light orange, R_f = 0.72) was in trace amounts and could not be isolated. The contents of the second band (orange, R_f = 0.61) were identified as MoIr$_3$(μ-CO)$_3$(CO)$_6$(PPh$_3$)$_2$(η-C$_5$H$_5$) (44.9 mg, 0.030 mmol, 78%) by solution IR and ^{1}H NMR spectroscopy.

X-ray Crystallographic Studies. General Methods. Crystals suitable for X-ray structural studies were grown by liquid diffusion of EtOH into CH_2Cl_2 solutions of the clusters at 3 °C. A single crystal was glued to a glass fiber and mounted on either a Rigaku AFC6S diffractometer (**3c**) or Nonius KappaCCD diffractometer (**3d**, **4d**, **5c**,**d**). The data acquisition and structural refinement details are summarized in Table 1. Aspects of the solution and refinement were handled within the CRYSTALS[18] or teXsan[19] software packages. The structures were solved by direct methods and expanded using difference Fourier techniques. Non-hydrogen atoms were refined anisotropically, and organic hydrogen atoms were included in idealized positions that were frequently recalculated. The final cycles of full-matrix least-squares refinement on *F* were based on N_{obs} reflections ($I > n\sigma(I)$) and converged to *R* and R_w.

3d. The crystallographic asymmetric unit consists of three independent molecules of the pentanuclear cluster. Anisotropic displacement parameters for the atoms of one pentamethylcyclopentadienyl group refined to unreasonable values. Each of these atoms was therefore split over two sites of half-occupancy. A connectivity was established to yield two orientations of the substituted five-membered ring. Isotropic displacement parameters were used with constraints where appropriate, and restraints were imposed on C−C distances and angles and on the planarities of the inner and outer C atoms. The relative populations of the two orientations were later refined. The cluster-bound hydrides were not observed directly in difference electron density maps, but their presence could be inferred from the positions of the other ligands. They were included at anticipated locations and refined positionally with restraints on M−H distances. The calculated esd's associated with the hydride atoms (Supporting Information) are smaller than might have been expected in a structure with so many heavy atoms and arise from the use of the restraints. The absolute structure was established by refinement of a Flack parameter. The biggest peak in the final difference electron density map was located near Ir atoms of molecule two.

4d. Partially overlapped twinned reflections in the X-ray diffraction pattern exist, the extent of the overlap being a function of *h*; this was refined using the constrained least-squares refinement

(18) Watkin, D. J.; Prout, C. K.; Carruthers, J. R.; Betteridge, P. W.; Cooper, R. I. *CRYSTALS Issue 11*; Chemical Crystallography Laboratory: Oxford, U.K., 2001.

(19) *teXsan: Single Crystal Structure Analysis Software*, version 1.8; Molecular Structure Corp.: The Woodlands, TX, 1997.

program RAELS96,[20] details of which are given in the Supporting Information. The crystallographic asymmetric unit consists of three cluster molecules. Hydrogen atoms of the methyl groups were included as sites of half occupancy with C−C−C−H torsion angles 60° apart, and the cluster-bound hydrides were included at idealized positions. The biggest peaks in the final difference electron density map are located within the clusters.

5c. The crystallographic asymmetric unit consists of one cluster molecule, with all atoms in general positions. The molecule has an approximate mirror plane running through it at $x = 1/4$. The methyl hydrogens were oriented to best-fit peaks observed in a difference electron density map. The largest peak observed in a subsequent difference map was found in the position expected for the hydride. H(1) was included at this location and refined positionally. Its precision is quite low, as expected in the presence of so many heavy atoms. The biggest peaks in the final difference electron density map are located near Ir atoms.

5d. The crystallographic asymmetric unit consists of half of a cluster molecule, with the remaining atoms being generated by a crystallographic mirror plane at $x = 1/4$. Anisotropic displacement parameters for the atoms of the pentamethylcyclopentadienyl group refined to unreasonable values. Each of these atoms was therefore split over two sites of half-occupancy. A connectivity was established to yield two orientations of the substituted five-membered ring which retained the crystallographic mirror plane. Isotropic displacement parameters were used with constraints where appropriate, and restraints were imposed on C−C distances and angles. The largest peak observed in a subsequent difference map was found in the position expected for the hydride. H(1) was included at this location and refined positionally with weak restraints on M−H distances. Its precision is quite low, as expected in the presence of so many heavy atoms. The biggest peaks in the final difference electron density map are located near Ir atoms and within the disordered methyl groups.

Electrochemical Study. The cyclic voltammogram of **3c** was recorded using a MacLab 400 interface and MacLab potentiostat from ADInstruments. The supporting electrolyte was 0.25 M $(NBu^n_4)PF_6$ in distilled, deoxygenated CH_2Cl_2. A solution containing ca. 2×10^{-3} mol L^{-1} complex was maintained under argon. The measurement was carried out using a platinum disc working, platinum auxiliary, and Ag/AgCl reference electrode, using the ferrocene/ferrocenium redox couple as an internal reference (0.56 V).

Theoretical Methods. Density functional theory calculations were executed in this study using the Amsterdam Density Functional (ADF) program, version ADF 2002.03,[21] developed by Baerends et al.[22] Calculations were performed on Linux-based Pentium IV computers or in parallel mode on the AlphaSever supercomputer

Chart 1

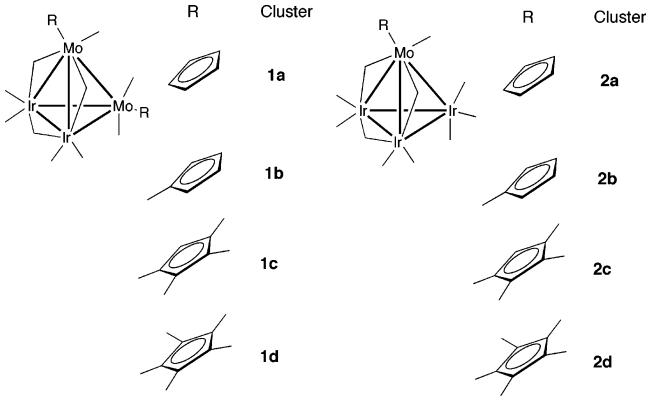

housed at the ANU Supercomputer Facility and operated under the Australian Partnership for Advanced Computing.

Calculations were performed in C_s symmetry. Electrons in orbitals up to and including 1s {C, O}, 3d {Mo}, and 4d {Ir} were treated in accordance with the frozen-core approximation. Geometry optimizations employed the local density approximation (LDA) to the exchange potential and the correlation potential of Vosko, Wilk, and Nusair (VWN),[23] in some cases featuring also the nonlocal corrections of Perdew, Burke, and Enzerhof (PBE).[24] In all calculations, the (Slater type orbital) basis sets used were of triple-ζ-plus-polarization quality for each atom; these basis sets are described as "TZP". All calculations were spin-restricted.

Relativistic corrections to the local density approximation were effected through single-point calculations employing the ZORA scalar relativistic correction,[25] using basis sets analogous to those employed in the geometry optimization calculations. In these relativistic corrections, correlation was addressed through the use of VWN,[23] PBE,[24] Becke−Perdew (BP),[26,27] and Becke−Lee−Yang−Parr (B−LYP)[26,28] functionals. We have previously found,[14] as have others,[29] that the VWN parametrization of the local density approximation delivers significantly better metal−metal and metal−ligand bond lengths for metal carbonyl clusters than are attained when nonlocal functionals (e.g., B−LYP) are employed for optimization; nevertheless, incorporation of nonlocal and relativistic corrections is generally considered to yield more accurate total and relative energies.

Results and Discussion

Syntheses and Spectroscopic Characterization. We previously reported the tetrahedral mixed molybdenum−iridium clusters **1a**−**d** and **2a**−**d** (Chart 1) and homologous tungsten−iridium clusters.[14] During a preparation of one of these clusters, namely $Mo_2Ir_2(\mu\text{-}CO)_3(CO)_7(\eta\text{-}C_5HMe_4)_2$ (**1c**) from $IrCl(CO)_2(4\text{-}NH_2C_6H_4Me)$ and excess $Li[Mo(CO)_3(\eta\text{-}C_5HMe_4)]$, the reaction mixture was left longer than usual prior to workup, and an extra band not previously encountered was present in the subsequent thin-layer chromatogram.

(20) Rae, A. D. *RAELS96: A Comprehensive Constrained Least-Squares Refinement Program*; Australian National University: Canberra, Australia, 1996.
(21) Baerends, E. J.; Bérces, A.; Bo, C.; Boerrigter, P. M.; Cavallo, L.; Deng, L.; Dickson, R. M.; Ellis, D. E.; Fan, L.; Fischer, T. H.; Fonseca Guerra, C.; van Gisbergen, S. J. A.; Groeneveld, J. A.; Gritsenko, O. V.; Harris, F. E.; van den Hoek, P.; Jacobsen, H.; van Kessel, G.; Kootstra, F.; van Lenthe, E.; Osinga, V. P.; Philipsen, P. H. T.; Post, D.; Pye, C.; Ravenek, W.; Ros, P.; Schipper, P. R. T.; Schreckenbach, G.; Snijders, J. G.; Sola, M.; Swerhone, D.; te Velde, G.; Vernooijs, P.; Versluis, L.; Visser, O.; van Wezenbeek, E.; Wiesenekker, G.; Wolff, S. K.; Woo, T. K.; Ziegler, T. *ADF 2002.03*; S.C.M., Theoretical Chemistry, Vrije Universiteit: Amsterdam, The Netherlands, http://www.scm.com, 2004.
(22) (a) te Velde, G.; Bickelhaupt, F. M.; Baerends, E. J.; Guerra, C. F.; van Gisbergen, S. J. A.; Snijders, J. G.; Ziegler, T. *J. Comput. Chem.* **2001**, *22*, 931. (b) Fonseca Guerra, C. F.; Snijders, J. G.; te Velde, G.; Baerends, E. J. *Theor. Chem. Acc.* **1998**, *99*, 391.
(23) Vosko, S. H.; Wilk, L.; Nusair, M. *Can. J. Chem.* **1980**, *58*, 1200.
(24) Perdew, J. P.; Burke, K.; Ernzerhof, M. *Phys. Rev. Lett.* **1996**, *77*, 3865.
(25) (a) van Lenthe, E.; Baerends, E. J.; Snijders, J. G. *J. Chem. Phys.* **1993**, *99*, 4597. (b) van Lenthe, E.; Ehlers, A. E.; Baerends, E. J. *J. Chem. Phys.* **1999**, *110*, 8943.
(26) Becke, A. D. *Phys. Rev. A* **1988**, *38*, 3098.
(27) Perdew, J. P. *Phys. Rev. B* **1986**, *33*, 8822.
(28) Lee, C.; Yang, W.; Parr, R. G. *Phys. Rev. B* **1988**, *37*, 785.
(29) Besançon, K.; Laurenczy, G.; Lumini, T.; Roulet, R.; Bruyndonckx, R.; Daul, C. *Inorg. Chem.* **1998**, *37*, 5634.

Scheme 1. Syntheses of $Mo_2Ir_3(\mu_3\text{-H})(\mu\text{-CO})_2(CO)_9(\eta\text{-}C_5H_{5-n}Me_n)_2$ ($n = 4, 5$)

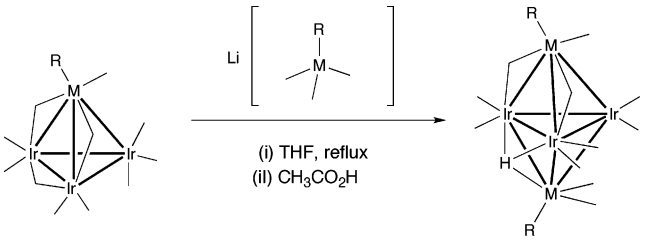

M	R	Product, yield
Mo		**3c**, 74 %
Mo		**3d**, 55 %
Mo		0 %
W		0 %

An X-ray structural study of a single-crystal obtained from the material present in this TLC band identified this minor product as the pentanuclear cluster $Mo_2Ir_3(\mu_3\text{-H})(\mu\text{-CO})_2(CO)_9(\eta\text{-}C_5HMe_4)_2$ (**3c**) (see below for structural study); it is assumed that an adventitious proton source (e.g., water on the TLC plates) is responsible for the cluster-bound hydride ligand. A small quantity of $MoIr_3(\mu\text{-CO})_3(CO)_8(\eta\text{-}C_5HMe_4)$ (**2c**) is known to be formed in this reaction[14] (its formation is also favored by higher temperatures), so reaction of this tetranuclear cluster with further $[Mo(CO)_3(\eta\text{-}C_5HMe_4)]^-$ was examined as a possible route to the dimolybdenum−triiridium pentanuclear cluster. Excess $Li[Mo(CO)_3(\eta\text{-}C_5HMe_4)]$ in THF reacts slowly at room temperature with **2c** (more rapidly at reflux) to afford, following protic workup, the core-expanded cluster **3c** in good yield (74%). Reaction of $MoIr_3(\mu\text{-CO})_3(CO)_8(\eta\text{-}C_5Me_5)$ (**2d**) with excess $Li[Mo(CO)_3(\eta\text{-}C_5Me_5)]$ proceeded similarly to afford $Mo_2Ir_3(\mu_3\text{-H})(\mu\text{-CO})_2(CO)_9(\eta\text{-}C_5Me_5)_2$ (**3d**), but the related cyclopentadienylmolybdenum and -tungsten reactions failed to give the analogous products (Scheme 1).

The complexes were characterized by IR, ^{1}H-NMR, and UV−vis (**3d**) spectroscopies, SI mass spectrometry, and single-crystal X-ray diffraction studies. The solution IR spectra in CH_2Cl_2 contain six ν(CO) bands, four corresponding to terminally bound carbonyls (2047−1892 cm^{-1}) and the other two bands corresponding to carbonyl groups in bridging modes (1778−1746 cm^{-1}). The ^{1}H-NMR spectra contain resonances assigned to the various cyclopentadienyl groups and characteristic hydride protons at δ −5.49 (**3c**) and −5.44 (**3d**). The UV−vis absorption spectrum of **3d** shows a maximum at 359 nm and a tail (with shoulders) stretching well into the visible region, giving rise to the brown color of these clusters. Similarly featureless low-energy regions of the UV−vis spectra were observed with the previously mentioned tetrahedral clusters.[14] An intense molecular ion peak and fragment ion peaks corresponding to loss of all carbonyls (competitive with loss of H and Me) are detected in the SI mass spectra.

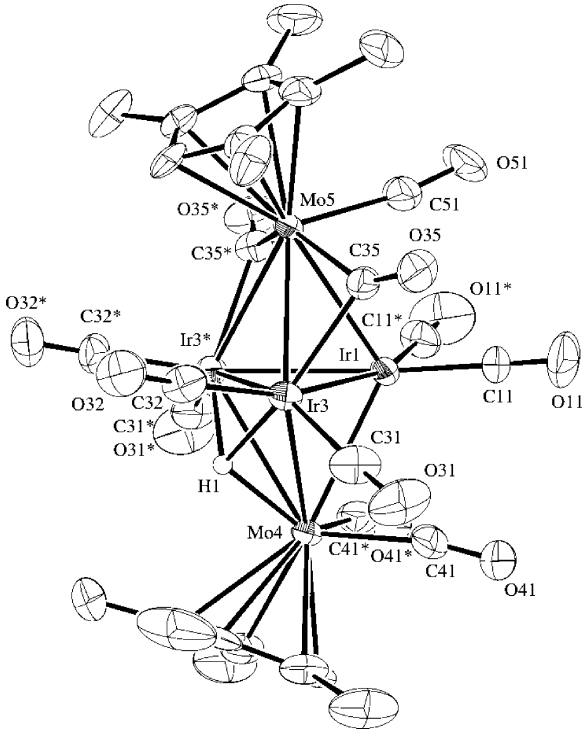

Figure 1. Molecular structure and atomic numbering scheme for $Mo_2Ir_3(\mu_3\text{-H})(\mu\text{-CO})_2(CO)_9(\eta\text{-}C_5HMe_4)_2$ (**3c**). Here and in Figures 2−5, displacement ellipsoids are shown at the 30% probability level. Hydrogen atoms have been omitted for clarity, with the exception of H1. The molecule lies on a mirror plane (passing through Ir1, Mo4, Mo5); the symmetry-expanded structure is shown.

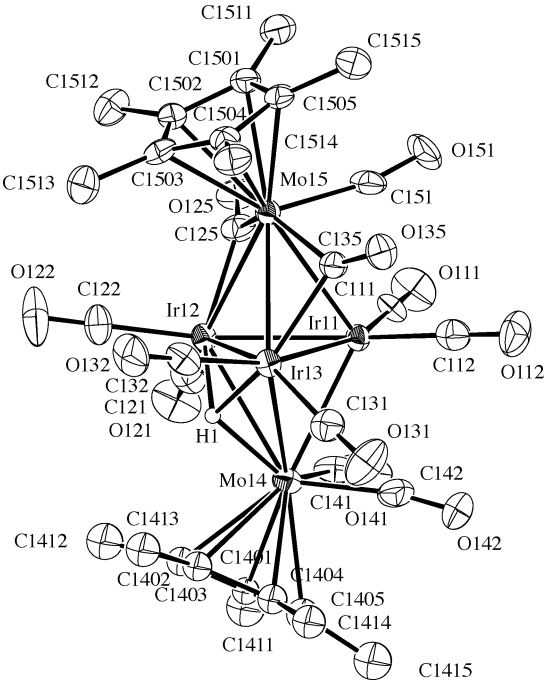

Figure 2. Molecular structure and atomic numbering scheme for $Mo_2Ir_3(\mu_3\text{-H})(\mu\text{-CO})_2(CO)_9(\eta\text{-}C_5Me_5)_2$ (**3d**). Hydrogen atoms have been omitted for clarity, with the exception of H1.

Related reactions employing excess carbonylmetalates with differing cyclopentadienyl ligands from the cluster precursor were then examined (Scheme 2). Reactions proceeded slowly

Scheme 2. Syntheses of $M_2Ir_3(\mu_3\text{-H})(\mu\text{-CO})_2(CO)_9(\eta\text{-}C_5H_{5-m}Me_m)(\eta\text{-}C_5H_{5-n}Me_n)$ (M = Mo, W; m = 0, 4; n = 4, 5) and $M_2Ir_3(\mu_3\text{-H})(\mu\text{-CO})_2(CO)_9(\eta\text{-}C_5H_{5-n}Me_n)_2$ (M = Mo, W; n = 4, 5)

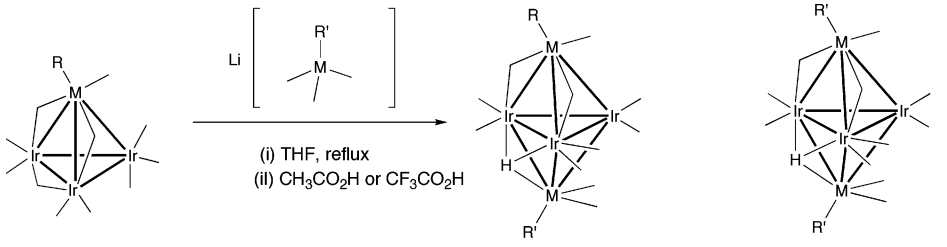

A B

M	R	R'	Product A, yield	Product B, yield
Mo			**5c**, 9 %	**3c**, 81 %
Mo			**5d**, 4 %	**3d**, 60 %
Mo			0 %	0 %
W			**6d**, 5 %	**4d**, 5 %

in CH_2Cl_2 or THF at room temperature but at a significantly accelerated rate at reflux in THF to afford, following protic workup, pentanuclear clusters with two identical cyclopentadienyl ligands in fair to excellent yield (B) and related mixed-cyclopentadienyl ligand-containing clusters (A) in lower yield. The core expansion reaction involving $Li[Mo(CO)_3(\eta\text{-}C_5HMe_4)]$ gave higher yields than the analogous reaction involving $Li[Mo(CO)_3(\eta\text{-}C_5Me_5)]$, and the latter proceeded to afford a much higher yield of the bis(pentamethylcyclopentadienyl)-containing product than the related reaction with the tungsten-containing precursor cluster and carbonylmetalate, which gave a large number of uncharacterized byproducts in low yield; no reactions employing cyclopentadienylcarbonylmetalate reagents afforded related products. Reaction between $Mo_2Ir_2(\mu\text{-CO})_3(CO)_7(\eta\text{-}C_5H_5)_2$ (**1a**) and $Li[Mo(CO)_3(\eta\text{-}C_5Me_5)]$ also did not afford any tractable products and was not pursued further. The new clusters were characterized by a combination of solution IR and ^{1}H NMR spectroscopies, SI or FAB mass spectrometry, and, in the case of **4d** and **5c**,**d**, single-crystal X-ray structural studies (see below). The solution IR spectra of the unsymmetrical compounds in CH_2Cl_2 contain five or six ν(CO) bands, four corresponding to terminally bound carbonyls and one or two corresponding to edge-bridging modes, the ^{1}H NMR spectra contain resonances in the methyl and cyclopentadienyl ring proton regions as well as one corresponding to a metal bound hydride [δ −5.44 to −5.63 (Mo-containing clusters), −1.83 (**4d**), and −2.00 (**6d**) (W-containing clusters)], and an intense molecular ion peak followed by fragment ion peaks corresponding to successive loss of carbonyls is observed in the mass spectra.

X-ray Structural Studies of 3c,d, 4d, and 5c,d. Single-crystal X-ray diffraction studies were carried out, confirming the molecular compositions. Figures 1−5 show ORTEP plots with the molecular structure and atomic labeling schemes; Table 1 contains crystallographic data acquisition and refinement parameters, and Table 2 lists selected bond distances.

The molecules of **3c** and **5d** lie on mirror planes passing through Ir1, Mo4, and Mo5. The other structures possess an approximate mirror plane in the same place and share the common trigonal bipyramidal core geometry with group 6 metal atoms in the apex sites and a triangle of iridium atoms defining the equatorial plane. M5 in all structures is ligated by the least bulky cyclopentadienyl group which sits across the (approximate) mirror plane, one terminal carbonyl, and two edge-bridging carbonyls arranged about a MIr_2 face. A face-capping hydride is positioned beneath the MIr_2 face and completes a "plane of bridging ligands" similar to the tetrahedral precursor cluster's "plane of bridging carbonyls."[30] M4 in all structures is ligated by a tetramethyl- or pentamethylcyclopentadienyl group which also sits across the mirror plane and two terminal carbonyls and shares in the face-capping hydride. The remaining carbonyls are coordinated in a terminal manner, two to each of the iridium atoms. The spectroscopically identifiable hydride was assigned to the Mo(4)Ir(3)Ir(3*) face in **3c** on the basis of potential energy calculations[31] and the observation that metal−metal bond lengths around the hydride-capped face

(30) Usher, A. J.; Dalton, G. T.; Lucas, N. T.; Waterman, S. M.; Petrie, S.; Stranger, R.; Humphrey, M. G.; Willis, A. C. *J. Organomet. Chem.* **2004**, *689*, 50.

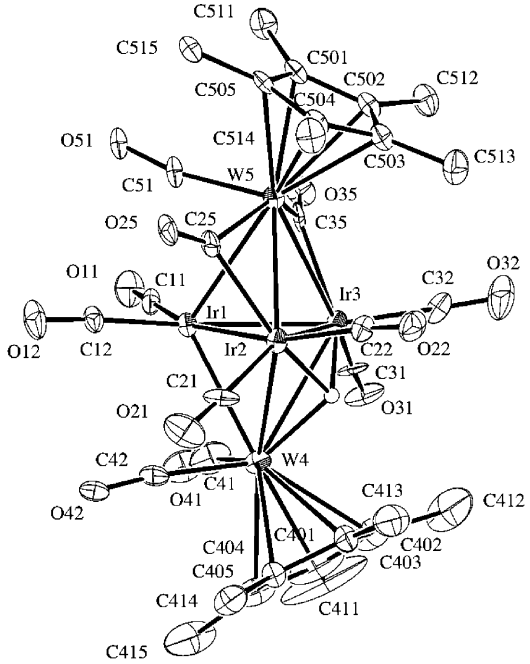

Figure 3. Molecular structure and atomic labeling scheme for one of three independent molecules of $W_2Ir_3(\mu_3\text{-H})(\mu\text{-CO})_2(CO)_9(\eta\text{-}C_5Me_5)_2$ (**4d**). Hydrogen atoms have been omitted for clarity, with the exception of the hydride.

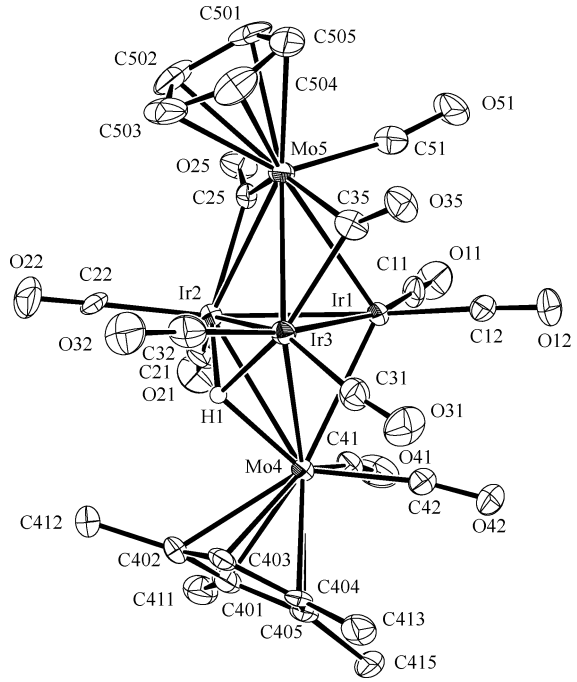

Figure 4. Molecular structure and atomic numbering scheme for $Mo_2Ir_3(\mu_3\text{-H})(\mu\text{-CO})_2(CO)_9(\eta\text{-}C_5H_5)(\eta\text{-}C_5HMe_4)$ (**5c**). Hydrogen atoms have been omitted for clarity, with the exception of H1.

are the longest of their respective bond types in the molecule; it was located crystallographically in **5c**,**d** and found to occupy the expected site. The carbonyls CO41/CO42 on M4 have some semibridging character which likely serves to redistribute electron density from the hydride-coordinating M4 to Ir1 which has only 17 e by formal electron counting

(31) (a) Orpen, A. G. *J. Chem. Soc. Dalton Trans.* **1980**, 2509. (b) Orpen, A. G., *HYDEX: A Program for Locating Hydrides in Metal Complexes*; University of Bristol: Bristol, U.K., 1999.

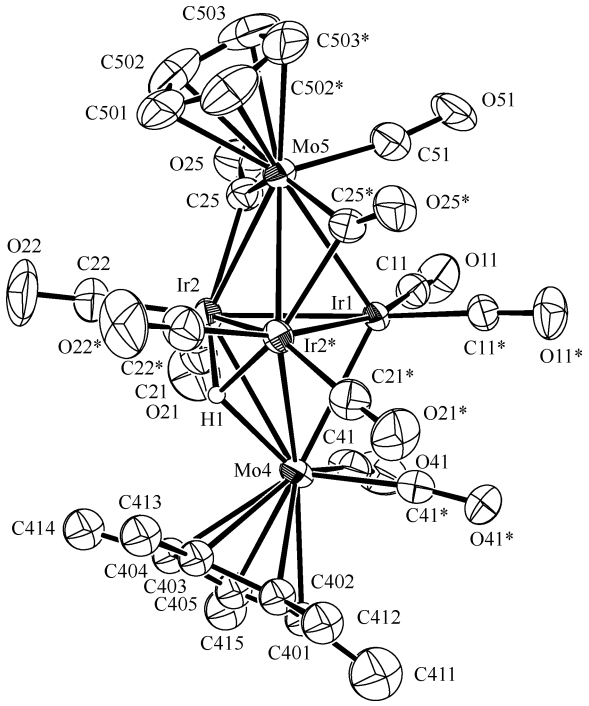

Figure 5. Molecular structure and atomic numbering scheme for $Mo_2Ir_3(\mu_3\text{-H})(\mu\text{-CO})_2(CO)_9(\eta\text{-}C_5H_5)(\eta\text{-}C_5Me_5)$ (**5d**). Hydrogen atoms have been omitted for clarity, with the exception of H1. The molecule lies on a mirror plane (passing through Ir1, Mo4, Mo5); the symmetry-expanded structure is shown.

rules. Ir2 and Ir3 are electron rich due to the presence of the bridging hydride. Electron counting reveals that the clusters have 72 valence electrons, precise for trigonal bipyramidal clusters.

Only one pentametallic mixed group 6−group 9 cluster with a trigonal bipyramidal geometry has been structurally characterized previously, namely $Mo_2Co_3(\mu_3\text{-S})_2(\mu\text{-CO})(CO)_6(\eta\text{-}C_5H_5)_2$,[32] with the cyclopentadienyl-ligated molybdenums in equatorial sites. This is in contrast to the present clusters in which the molybdenum atoms occupy the less sterically hindered apical sites; the metal carbonyl anion precursor could in principle add to a $MoIr_2$ face of the tetrahedral precursors, rather than the Ir_3 face, resulting in a trigonal bipyramid with one Mo atom in an equatorial site and the other in an apical site. The regioselectivity in the present case may, in part, be due to the presence of reactants with the bulkier highly methylated cyclopentadienyl groups.

Electrochemical Study. The cyclic voltammogram of $Mo_2Ir_3(\mu_3\text{-H})(\mu\text{-CO})_2(CO)_9(\eta\text{-}C_5HMe_4)_2$ (**3c**) contains a single irreversible oxidation (D; $E_p = 0.86$ V) and irreversible reduction (A, $E_p = -1.06$ V) with associated daughter peaks B and C (Figure 6). The peak height comparison is consistent with the oxidation process involving the transfer of more electrons than the reduction process, although the stoichiometry has not been ascertained by coulometry. The separation of the oxidation and reduction processes [$E_p(\text{ox}) - E_p(\text{red}) = 1.92$ V] is less than that observed for any of the related tetranuclear clusters [$E_p(\text{ox}) - E_p(\text{red}) = 2.04-2.56$ V];[14] this may correlate with a closer spacing of the HOMO−

(32) Li, P.; Curtis, D. *Inorg. Chem.* **1990**, *29*, 1242.

Table 2. Selected Bond Lengths (Å) for **3c**,**d**, **4d**, and **5c**,**d**

param	**3c**: M = Mo[a]	**3d**: M = Mo[b]	**4d**: M = W[b]	**5c**: M = Mo	**5d**: M = Mo[a]
Ir1−Ir2	2.6808(5)	2.6874(5), 2.6646(4), 2.6777(5)	2.678(1), 2.691(1), 2.674(1)	2.6748(4)	2.6716(4)
Ir1−Ir3	2.6808(5)	2.6799(5), 2.6959(4), 2.6736(5)	2.685(1), 2.663(1), 2.675(1)	2.6698(4)	2.6716(4)
Ir1−M4	2.760(1)	2.7737(8), 2.7731(8), 2.7702(8)	2.752(2), 2.751(1), 2.751(4)	2.7767(6)	2.7735(9)
Ir1−M5	2.871(1)	2.8947(8), 2.9000(8), 2.9007(8)	2.877(1), 2.878(1), 2.880(1)	2.8851(7)	2.889(1)
Ir2−Ir3	2.7241(6)	2.7565(4), 2.7603(4), 2.7785(8)	2.760(1), 2.765(1), 2.780(1)	2.7554(4)	2.7643(5)
Ir2−M4	2.9211(9)	2.9115(9), 2.9197(8), 2.8907(8)	2.885(2), 2.909(1), 2.905(1)	2.9226(7)	2.9070(9)
Ir2−M5	2.839(1)	2.8323(8), 2.8491(8), 2.8406(8)	2.819(1), 2.842(1), 2.832(1)	2.8350(7)	2.8310(8)
Ir3−M4	2.9211(9)	2.9075(9), 2.9162(8), 2.9235(8)	2.899(2), 2.897(1), 2.880(1)	2.8824(7)	2.9070(9)
Ir3−M5	2.839(1)	2.8292(8), 2.8472(8), 2.8465(8)	2.823(2), 2.837(1), 2.832(1)	2.8300(7)	2.8310(8)
Ir2−C25	2.148(9)	2.10(1), 2.126(9), 2.118(9)	2.12(2), 2.14(2), 2.18(2)	2.13(1)	2.111(8)
M5−C25	2.124(9)	2.16(1), 2.146(9), 2.141(9)	2.09(2), 2.14(2), 2.08(2)	2.117(9)	2.135(8)
Ir3−C35	2.148(9)	2.110(9), 2.112(9), 2.152(9)	2.12(2), 2.14(2), 2.17(2)	2.07(1)	2.111(8)
M5−C35	2.124(9)	2.141(9), 2.163(9), 2.100(9)	2.10(2), 2.12(2), 2.11(2)	2.17(1)	2.135(8)

[a] Crystallographic mirror plane. Asterisked labels in the ORTEP diagrams correspond to symmetry-expanded atoms that have been relabeled in this table for consistency and ease of comparison. [b] 3 molecules in the asymmetric unit.

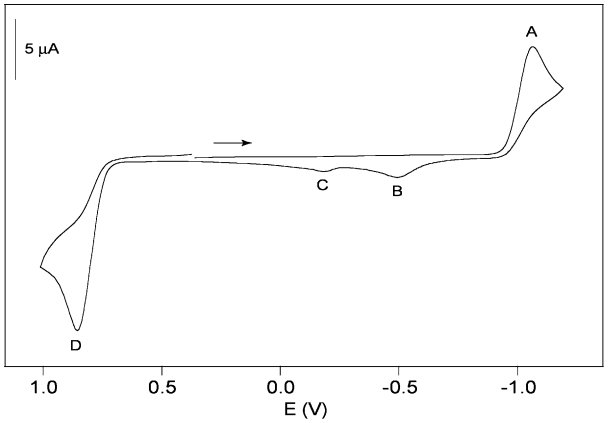

Figure 6. Cyclic voltammogram of $Mo_2Ir_3(\mu_3\text{-}H)(\mu\text{-}CO)_2(CO)_9(\eta\text{-}C_5HMe_4)_2$ (**3c**) at room temperature.

LUMO energy levels in the pentanuclear cluster **3c**, as expected when progressing to higher nuclearity clusters.

Studies to Elucidate the Mechanism. From the reactions described above, several observations can be made. Core expansion reactions involving $Li[Mo(CO)_3(\eta\text{-}C_5HMe_4)]$ gave uniformly higher yields than analogous reactions involving $Li[Mo(CO)_3(\eta\text{-}C_5Me_5)]$, possibly due to the less sterically hindered tetramethylcyclopentadienyl group projecting the unsubstituted vertex of the cyclopentadienyl ring down the face of the cluster. The formation of the homovertex clusters $Mo_2Ir_3(\mu_3\text{-}H)(\mu\text{-}CO)_2(CO)_9(\eta\text{-}C_5HMe_4)_2$ (**3c**) and $Mo_2Ir_3(\mu_3\text{-}H)(\mu\text{-}CO)_2(CO)_9(\eta\text{-}C_5Me_5)_2$ (**3d**) from the cyclopentadienyl-containing precursor $MoIr_3(\mu\text{-}CO)_3(CO)_8(\eta\text{-}C_5H_5)$ (**2a**) is consistent with the core expansion process not being a simple addition of a molybdenum-containing fragment to the triangle of iridium atoms of the parent cluster but rather that a mechanism involving core expansion and vertex replacement is operative. Simple ligand exchange of a cyclopentadienyl group for a highly methylated cyclopentadienyl group is unlikely, due to the large energetic barrier to dissociative exchange and steric barrier to associative exchange. [Note that formal cyclopentadienyl transfer from molybdenum to cobalt, displacing CO ligands, has been reported but required extended reaction and proceeded in low yield: $MoCo_2(\mu_3\text{-}CMe)(CO)_8(\eta\text{-}C_5H_5)$ reacts with $Mo_2(CO)_6(\eta\text{-}C_5H_5)_2$ in refluxing benzene for 6 days to afford $MoCo_3(\mu_3\text{-}CMe)(\mu\text{-}CO)_2(CO)_7(\eta\text{-}C_5H_5)_2$ in 5% yield.[33]] Although vertex replacement could be distinguished from ligand exchange in the current study by isotopically labeling a molybdenum vertex, this presents significant practical difficulties, so the related reaction with another group 6 metal, tungsten, was attempted (Scheme 3).

Scheme 3. Attempted Synthesis of a Heterotrimetallic Cluster

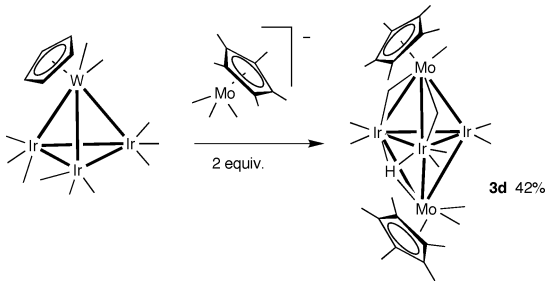

The lower yield of **3d** obtained from the reaction of $WIr_3(CO)_{11}(\eta\text{-}C_5H_5)$ with $Li[Mo(CO)_3(\eta\text{-}C_5Me_5)]$ is consistent with the lower yield of **4d** from the tungsten−triiridium precursor (see above). More importantly, the complete absence of the heterotrimetallic cluster $MoWIr_3(\mu_3\text{-}H)(\mu\text{-}CO)_2(CO)_9(\eta\text{-}C_5Me_5)(\eta\text{-}C_5H_5)$ is consistent with vertex replacement being a fundamental step in the core expansion process.

As was mentioned above, reaction of $MoIr_3(\mu\text{-}CO)_3(CO)_8(\eta\text{-}C_5H_5)$ (**2a**) with $Na[Mo(CO)_3(\eta\text{-}C_5H_5)]$ failed to afford $Mo_2Ir_3(\mu_3\text{-}H)(\mu\text{-}CO)_2(CO)_9(\eta\text{-}C_5H_5)_2$. Because $Mo_2Ir_3(\mu_3\text{-}H)(\mu\text{-}CO)_2(CO)_9(\eta\text{-}C_5H_5)(\eta\text{-}C_5Me_5)$ (**5d**) is experimentally accessible via addition of $Li[Mo(CO)_3(\eta\text{-}C_5Me_5)]$ to $MoIr_3(\mu\text{-}CO)_3(CO)_8(\eta\text{-}C_5H_5)$ (**2a**), a target compound known to be thermodynamically stable [unlike $Mo_2Ir_3(\mu_3\text{-}H)(\mu\text{-}CO)_2(CO)_9(\eta\text{-}C_5H_5)_2$, which is unknown] is available with which to objectively test the ability of the $Na[Mo(CO)_3(\eta\text{-}C_5H_5)]$ fragment to core-expand a cluster, the result from which is shown in Scheme 4. The inability of $Na[Mo(CO)_3(\eta\text{-}C_5H_5)]$ to form **5d** by core-expansion of **2d** is therefore due solely to the use of the $\eta\text{-}C_5H_5$ ligand rather than the $\eta\text{-}C_5Me_5$ (or $\eta\text{-}C_5HMe_4$) ligand. Major differences between cyclopentadienyl and pentamethylcyclopentadienyl- (or tetramethylcyclopentadienyl-) containing species are both steric and

(33) Blumhofer, R.; Fischer, K.; Vahrenkamp, H. *Chem. Ber.* **1986**, *119*, 194.

Scheme 4. Alternative Routes into $Mo_2Ir_3(\mu_3\text{-}H)(\mu\text{-}CO)_2(CO)_9(\eta\text{-}C_5H_5)(\eta\text{-}C_5Me_5)$ (**5d**) Highlighting the Different Behavior of $[Mo(CO)_3(\eta\text{-}C_5Me_5)]^-$ and $[Mo(CO)_3(\eta\text{-}C_5H_5)]^-$

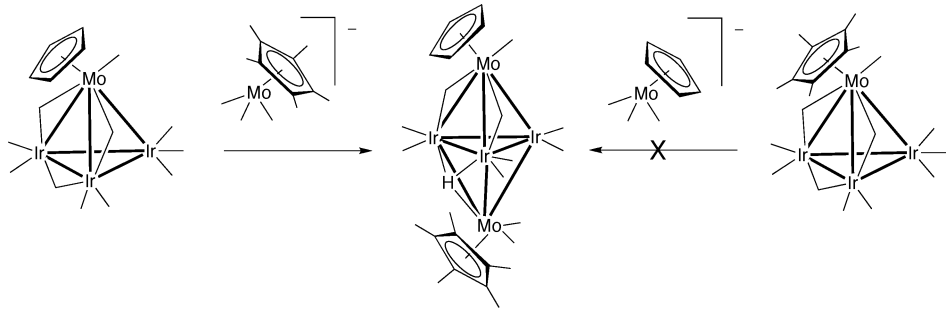

Scheme 5. Postulated Route to the Homoapex Cluster **3d**

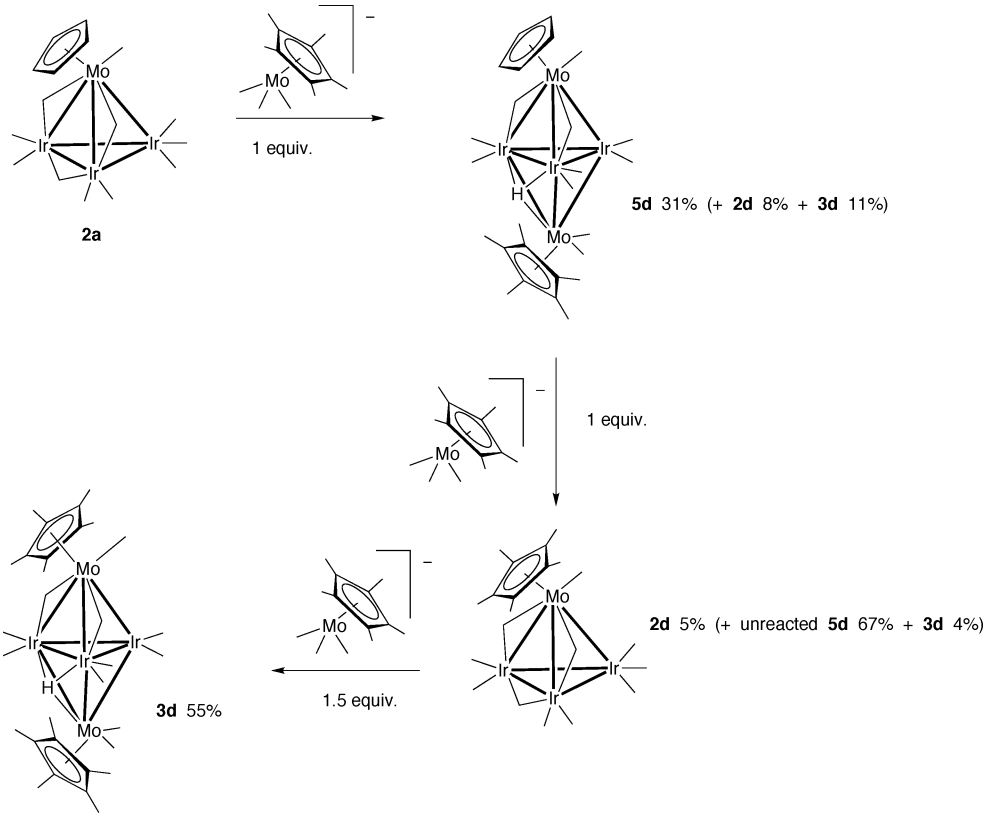

nucleophilic and are difficult to deconvolute, but the dominant factor governing the failure of this reaction is clearly not the thermodynamic instability of the expected product.

We then pursued the treatment of a tetrahedral cluster with 1 equiv of carbonylmetalate reagent. Reaction of $MoIr_3(\mu\text{-}CO)_3(CO)_8(\eta\text{-}C_5H_5)$ (**2a**) with 1 equiv of $Li[Mo(CO)_3(\eta\text{-}C_5Me_5)]$ affords the heteroapex cluster **5d** in 31% yield and the homoapex cluster **3d** in 11% yield but in addition the tetranuclear cluster $MoIr_3(\mu\text{-}CO)_3(CO)_8(\eta\text{-}C_5Me_5)$ (**2d**) in 8% yield; as was noted above, **2d** is not a precursor for **5d** but is for **3d**. The homoapex cluster **3c** was treated with excess $Li[Mo(CO)_3(\eta\text{-}C_5Me_5)]$ but returned unreacted **3c**, confirming the stability of the electron-rich and sterically shielded highly methylated homoapex pentanuclear clusters. In contrast, the heteroapex cluster **5d** reacts with 1 equiv of $Li[Mo(CO)_3(\eta\text{-}C_5Me_5)]$ to afford unreacted **5d** (67%) but in addition the homoapex cluster **3d** (4%) and the tetranuclear cluster **2d** (5%). Conversion of **2d** to **3d** has been established above (Scheme 1). These results permit the reaction sequence in Scheme 5 to be suggested as a route from the nonmethylated precursor **2a** to the homoapex clusters containing highly alkylated cyclopentadienyl ligands (**3c**,**d**), which are presumed to be the thermodynamically most stable species in this system (Scheme 5). Note that, in addition to the sequence in Scheme 5, the direct reaction of **2a** to afford **2d** (without the intermediacy of **5d**) or of **5d** to afford **3d** (without the intermediacy of **2d**) is not excluded by our synthetic studies.

We also explored possible core expansion/vertex replacement in this system with a ligand-substituted precursor cluster and a carbonylmetalate anion. The core expansion of a ligand-substituted cluster may be expected to display strong dependence on the steric requirements of the coordinated ligand so the small ligand Bu^tNC was identified as the most likely candidate to minimize ligand intervention in the core expansion process. Reaction of $MoIr_3(\mu\text{-}CO)_3(CNBu^t)(CO)_7(\eta\text{-}$

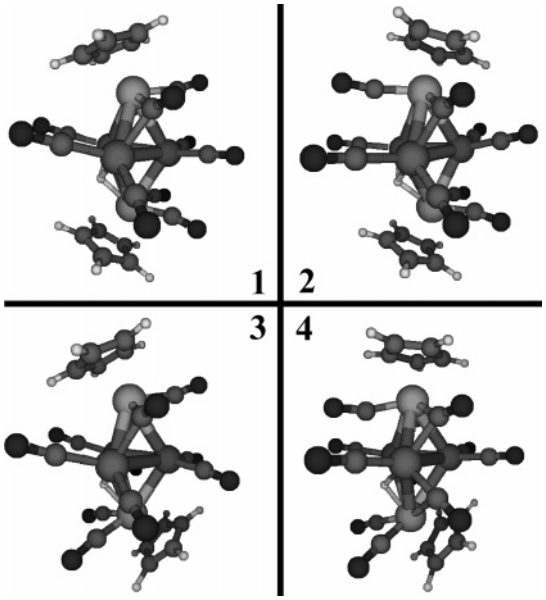

Figure 7. Optimized geometries of the four C_s-symmetry conformers possible for the bis(cyclopentadienylmolybdenum)-capped clusters, obtained at the VWN/TZP level of theory. The hydride-bearing faces are shown oriented toward the lower left of the metal cluster core.

C_5Me_5) with Li[$Mo(CO)_3(\eta$-$C_5Me_5)$] produces the unsubstituted cluster $Mo_2Ir_3(\mu_3$-$H)(\mu$-$CO)_2(CO)_9(\eta$-$C_5Me_5)_2$ (**3d**) in low yield, indicating that elimination of the Bu^tNC ligand is required for formation of the core-expanded cluster. Reactions of other ligand-substituted tetranuclear clusters with Li[$Mo(CO)_3(\eta$-$C_5Me_5)$] were not attempted. The capping fragments explored in the studies detailed above differ only in cyclopentadienyl ring substitution, viz. [$Mo(CO)_3$-$(\eta$-$C_5H_{5-n}Me_n)]^-$ (n = 0, 4, 5), for which a high degree of methylation results in successful core expansion. The ability of the bulkier, relatively more electron rich species to core expand the molybdenum/tungsten−triiridium clusters could potentially be mimicked by the addition of a bulky, strongly electron donating ligand to the [$Mo(CO)_3(\eta$-$C_5H_5)]^-$ anionic fragment. An attempted core expansion reaction combining excess K[$Mo(CO)_2(PPh_3)(\eta$-$C_5H_5)$] with $MoIr_3(\mu$-$CO)_3(CO)_8$-$(\eta$-$C_5H_5)$ yielded $MoIr_3(\mu$-$CO)_3(CO)_6(PPh_3)_2(\eta$-$C_5H_5)$ in 78% yield; no pentanuclear cluster was observed. Monitoring the reaction mixture by solution IR showed the simultaneous consumption of K[$Mo(CO)_2(PPh_3)(\eta$-$C_5H_5)$] and formation of K[$Mo(CO)_3(\eta$-$C_5H_5)$], indicating efficient ligand transfer between the anionic fragment and the cluster itself with minimal loss of CO; the high yield of $MoIr_3(\mu$-$CO)_3(CO)_6$-$(PPh_3)_2(\eta$-$C_5H_5)$ confirms this. Core expansion and ligand transfer represent two possible competing reactions in this system, ligand transfer being sterically favored and core expansion (with a non-CO ligand present) seemingly being strongly disfavored.

Theoretical Studies. Our DFT calculations on the pentanuclear Mo_2Ir_3 clusters pursued several objectives. First, we investigated the geometric isomerism of the clusters, using $Mo_2Ir_3(\mu_3$-$H)(\mu$-$CO)_2(CO)_9(\eta$-$C_5H_5)_2$ as a model. Calculations on the four feasible C_s-symmetric structures (see Figure 7 and Table 3), at various levels of theory, consistently show that the lowest energy configuration is that which, in accord with the crystalline geometry of the related pentamethylcyclopentadienyl-containing clusters, has both cyclopentadienyl ligands canted toward the hydride-bearing face of the cluster.

Calculations were also performed on the three possible pentamethylcyclopentadienyl-containing analogues of model structure 1 (see Figure 8 and Table 4). Two of these analogues (those with R′ = Me) correspond to isolated clusters **5d** and **3d**, while the third features the permethylated cyclopentadienyl on the opposite Mo atom. Geometric details of the optimized structures are reported in Table 4. It is apparent that PBE/TZP systematically overestimates the metal−metal bond lengths in these clusters by up to ∼0.2 Å, whereas the VWN/TZP calculations are uniformly within 0.1 Å of the crystallographic values. Experience has shown that VWN/TZP is much more prone to bond length *underestimation* than are any DFT methods, such as PBE, which include nonlocal corrections. It is therefore unlikely that other currently available density functionals can better characterize the cluster geometries. Note that both optimization approaches used here perform better in calculating metal−*ligand* separations (here illustrated by the distance between the cyclopentadienyl centroid and Mo) than in determining intermetallic distances.

Our optimizations at the VWN/TZP and PBE/TZP levels of theory show that there is no significant difference in total energy between the two structures **H/Me** (i.e., with R = H, R′ = Me) and **Me/H** (i.e., with R = Me, R′ = H). Both levels of theory return energy differences of <6 kJ mol^{-1} between these two isomers but differ as to which is the lower energy isomer. The inclusion of ZORA scalar relativistic corrections does not resolve this issue. Our calculations suggest that the isolation of structure **H/Me**, in preference to structure **Me/H**, does not reflect any significant thermochemical difference between the two isomers. If the observed location of pentamethylcyclopentadienyl (and, by analogy, tetramethylcyclopentadienyl) ligands within the isolated structures is not controlled by thermochemistry, then what is the mechanistic driving force at work?

One possible interpretation is that the mechanism depends on the reactivity of some precursor, in a manner that is sensitive to the degree of cyclopentadienyl ligand alkylation. The experimental studies show that $MoIr_3(\mu$-$CO)_3(CO)_8(\eta$-$C_5R_5)$ [R = H (**2a**), Me (**2d**)] yields a pentanuclear cluster with addition of $Mo(\eta$-$C_5Me_5)$ but not with addition of $Mo(\eta$-$C_5H_5)$. This may reflect the nucleophilicity of [$Mo(CO)_3$-$(\eta$-$C_5R'_5)]^-$ (R′ = H, Me). We have attempted to address this notion through DFT calculations. Vacuum-phase calculations on $M^+[Mo(CO)_3(\eta$-$C_5R'_5)]^-$ ($M^+ = Na^+$, NMe_4^+) show that there is a preference for M^+ cation coordination at the face bounded by the three CO ligands compared to the nonmetalated face of the cyclopentadienyl ring, consistent with the results from related solution studies.[34] This preference is *stronger* (by ∼10 kJ mol^{-1}) when the cyclopentadienyl ring is permethylated than when not. Taken by itself,

(34) Darensbourg, M. Y.; Jimenez, P.; Sackett, J. R.; Hanckel, J. M.; Kump, R. L. *J. Am. Chem. Soc.* **1982**, *104*, 1521.

Table 3. Relative Energies of the $Mo_2Ir_3(\mu_3\text{-}H)(\mu\text{-}CO)_2(CO)_9(\eta\text{-}C_5H_5)_2$ Geometric Isomers, Obtained from Density Functional Theory Calculations Using the TZP Basis Set for All Atoms

	E_{rel}/kJ mol^{-1} [a]							
	VWN opt geom						PBE opt geom	
struct	VWN	PBE	VWN + ZORA	PBE + ZORA	BP + ZORA	B−LYP + ZORA	PBE	PBE + ZORA
1	0	0	0	0	0	0	0	0
2	14	22	24	32	31	32	18	24
3	50	41	61	52	49	43	41	56
4	45	49	90	96	94	93	48	93

[a] Energy, expressed relative to the total energy of the lowest-energy stationary point, for calculations using the indicated density functional method. Optimizations were performed using the VWN or PBE functional (see text) and excluding relativistic corrections. Subsequent single-point calculations, including those using the ZORA protocol for scalar relativistic corrections, were performed upon the corresponding VWN- or PBE-optimized geometries.

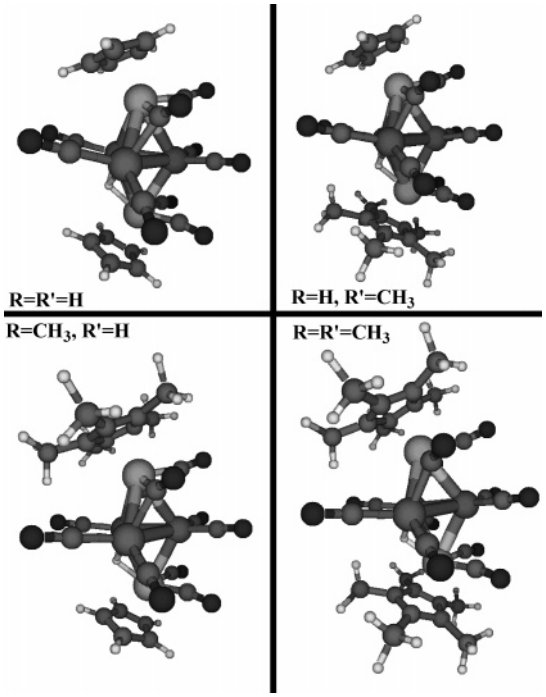

Figure 8. Optimized geometries, obtained at the VWN/TZP level of theory, of pentamethylcyclopentadienyl-derivatized analogues of the bis(cyclopentadienylmolybdenum)-capped cluster isomer **1** (Figure 6). Key bond lengths for these species are given in Table 4. The two structures on the right-hand side (i.e., with R′ = Me) are those that have been isolated crystallographically.

this result qualitatively supports the notion that the orientational dependence of nucleophilicity in $[Mo(CO)_3(\eta\text{-}C_5R'_5)]^-$ may be sensitive to the degree of cyclopentadienyl alkylation, in a manner consistent with the isolation of tetramethylcyclopentadienyl- and pentamethylcyclopentadienyl-containing pentanuclear complexes rather than those featuring only cyclopentadienyl, and of isolation of **H/Me** but not **Me/H**. However, it is doubtful that vacuum-phase calculations can yield results that are meaningful for a mechanistic discussion on the formation of these pentanuclear complexes, because our hypothesized nucleophiles $[Mo(CO)_3(\eta\text{-}C_5R'_5)]^-$ will necessarily be solvated in solution, an effect ignored in the calculations described above. We have performed single-point calculations on the "vacuum-optimized" M^+ $[Mo(CO)_3(\eta\text{-}C_5R'_5)]^-$ structures, using the COSMO protocol for inclusion of solvent corrections. These solvent-corrected calculations overturn the vacuum-phase trend: the most nucleophilic face of the precursor is now the cyclopentadienyl ring, with no significant effect seen arising from the level of cyclopentadienyl alkylation. Thus, the solvent-corrected calculations that we have performed do not satisfactorily illuminate the mechanism involved in pentanuclear cluster formation. Note, however, that some significant shortcomings remain in the method that we have used to attempt to address solvent effects. First, the use of vacuum-optimized single-point geometries neglects the real effective bulk of the solvated species M^+ and $[Mo(CO)_3(\eta\text{-}C_5R'_5)]^-$. Second, by not including explicit solvent molecules the modeled solvent field is likely insensitive to the hydrophobicity of the cyclopentadienyl alkyl groups, an effect which in reality could significantly influence the orientational dependence of nucleophilicity in the suggested precursor.

We conclude that while DFT is able to show that the mechanistic preference for **H/Me** over **Me/H** is not a thermodynamic effect, it is not able at present to satisfactorily clarify the pentanuclear clusters' mechanism of formation.

Discussion

The crystallographically observed disposition of ligands about the trigonal bipyramidal cluster cores corresponds to that predicted by DFT to be of lowest energy. The observed preference for hydride/bridging carbonyl disposition, cf. the cyclopentadienyl/pentamethylcyclopentadienyl-containing vertices in **5d**, could not be resolved by calculations. Such differences as exist at these vertices are particularly subtle; there is no significant difference in experimental bond lengths at the M5 vertex in **5d** and **3d**, despite the differing level of alkylation.

Information on core electron density variation across this series of clusters can be gleaned from ^{1}H NMR and IR spectroscopy, the spectroscopic data suggesting a systematic change upon modifying cluster composition. There is a decrease in $\nu(CO_t)$ values upon replacement of C_5H_5 by C_5HMe_4 (proceeding from **5c** to **3c**) or by C_5Me_5 (proceeding from **5d** to **3d** or **6d** to **4d**), and on replacing C_5HMe_4 by C_5Me_5 (proceeding from **3c** to **3d** or **5c** to **5d**), consistent with an increase in cluster core electron richness upon cyclopentadienyl alkylation. Progressive alkylation of cyclopentadienyl rings also results in a systematic downfield shift of the hydride ^{1}H NMR resonance in these clusters.

The present studies have also shed light on the mechanism of the cluster growth and metal exchange in this system. Mechanistic understanding of metal exchange in transition

Table 4. Key Bond Lengths (Å) and Bond Angles (deg) for {Mo[1](η-C_5R_5)}{Mo[2](η-$C_5R'_5$)}Ir_3(μ_3-H)(μ-CO)$_2$(CO)$_9$ (R, R′ = H, Me), Obtained from Optimizations at the VWN/TZP (in Parentheses, PBE/TZP) Level of Theory

param	R = R′ = H	R = H, R′ = Me	expt (**5d**)	R = Me, R′ = H	R = R′ = Me	expt (**3d**)
r(η-C_5R_5−Mo[1])	1.961 (2.021)	1.965 (2.017)	**1.963**	1.978 (2.046)	1.977 (2.044)	**1.998**
r(Mo[1]−Ir[1])	2.913 (3.034)	2.926 (3.036)	**2.889**	2.927 (3.049)	2.928 (3.054)	**2.895**
r(Mo[1]−Ir[2])	2.900 (2.989)	2.903 (2.987)	**2.831**	2.904 (3.002)	2.895 (3.002)	**2.831**
r(Ir[1]−Ir[2])	2.771 (2.819)	2.759 (2.803)	**2.672**	2.767 (2.814)	2.764 (2.805)	**2.684**
r(Ir[2]−Ir[2'])	2.825 (2.885)	2.845 (2.893)	**2.764**	2.852 (2.898)	2.851 (2.911)	**2.757**
r(Ir[1]−Mo[2])	2.844 (2.930)	2.841 (2.955)	**2.774**	2.766 (2.952)	2.849 (2.957)	**2.774**
r(Ir[2]−Mo[2])	2.950 (3.036)	2.947 (3.054)	**2.907**	2.943 (3.028)	2.938 (3.039)	**2.910**
r(Mo[1]−Mo[2])	4.846 (5.030)	4.852 (5.059)	**4.786**	4.857 (5.048)	4.838 (5.062)	**4.787**
r(Mo[2]−η-C_5R_5)	1.975 (2.028)	1.996 (2.054)	**2.009**	1.974 (2.028)	2.025 (2.051)	**1.998**
(η-C_5R_5Mo[1]Mo[2])	155.3 (153.6)	156.0 (152.9)	**150.7**	154.7 (156.1)	156.6 (155.6)	**154.1**
(Mo[1]Mo[2]-η-C_5R_5)	152.0 (149.4)	149.4 (148.7)	**145.3**	151.7 (147.8)	159.8 (148.1)	**146.4**

metal carbonyl cluster complexes has been summarized elsewhere.[4] Total fragmentation followed by recombination of fragments is an unusual route for high-yielding metal exchange because of the large number of possibilities for cluster reconstitution. The results from this study are not consistent with this pathway. Specifically, the absence of $Ir_4(CO)_{12}$ among the products mitigates against this possibility, as does the strength of Ir−Ir bonds, all three of which would need to be cleaved in the tetrahedral precursor. Monometallic fragment elimination followed by fragment addition or fragment addition followed by fragment elimination are the vertex replacement procedures for which most evidence is extant with lower nuclearity clusters. While elimination followed by addition cannot be ruled out as a possibility for at least some of the product distribution in the present studies (for example, for formation of **2d** from **2a**), it cannot account for the formation of the "mixed" clusters such as **5d**. Results from the present study are consistent with successive fragment addition and elimination steps. While being mindful of the low yields, this is a rare example of the step-by-step progression through such a cycle and the first for a medium-nuclearity cluster, one unsupported by main group atom vertices and one driven by ligand rather than metal variation, particularly noteworthy being the high yields of the homoapex clusters **3c**,**d** from **2a** following this sequence of mechanistic steps.

Acknowledgment. We thank the Australian Research Council (ARC) for financial support (M.G.H., R.S.) and Johnson-Matthey Technology Center for the generous loan of iridium salts (M.G.H.). M.G.H. holds an ARC Australian Professorial Fellowship, and N.T.L. was an Australian Postgraduate Awardee.

Supporting Information Available: Crystallographic files (CIF). This material is available free of charge via the Internet at http://pubs.cas.org.

IC061736L